Design of active debris flow mitigation measures: a comprehensive analysis of existing impact models

DESIGN OF ACTIVE DEBRIS FLOW MITIGATION MEASURES: A COMPREHENSIVE ANALYSIS OF EXISTING IMPACT MODELS

Federico Vagnon
Department of Earth Science, University of Turin, Via Valperga Caluso 35, 10125, Turin, Italy
email: federico.vagnon@unito.it - Tel: +39 0116705325
ORCID: 0000-0003-0539-0557

Abstract:
Debris flows occur in mountainous areas characterized by steep slope and occasional severe rainstorms. The massive urbanization in these areas raised the importance of studying and mitigating these phenomena. Concerning the strategy of protection, it is fundamental to evaluate both the effect of the magnitude (that concerns the definition of the hazard), in terms of mobilized volume and travel distance, and the best technical protection structures (that concerns the mitigation measures) to reduce the existing risk to an acceptable residual one. In particular, the mitigation measure design requires the evaluation of the effects of debris flow impact forces against them. In other words, once it is established that mitigation structures are required, the impacting pressure shall be evaluated and it should be verified that it does not exceed barrier resistance.
In this paper the author wants to focus on the definition and the evaluation of the impacting load of debris flows on protection structures: a critical review of main existing models and equations treated in scientific literature is here presented. Although most of these equations are based on solid physical basis, they are always affected by an empirical nature due to the presence of coefficients for fitting the numerical results with laboratory and, less frequently, field data. The predicting capability of these equations, namely the capability of fitting experimental/field data, is analysed and evaluated using ten different datasets available in scientific literature. The purpose of this paper is to provide a comprehensive analysis of the existing debris flow impact models, highlighting their strong points and limits. Moreover, this paper could have a practical aspect by helping engineers in the choice of the best technical solution and the safe design of debris flow protection structures. Existing design guidelines for debris flow protection barrier have been analysed. Finally, starting from the analysis of the hydro-static model response to fit field data and introducing some practical assumptions, an empirical formula is proposed for taking into account the dynamic effects of the phenomenon.

Keywords: debris flow, impact models, landslide-structure interaction, predicting capability

INTRODUCTION

In the last decades, the climate changes have rapidly triggered the glacier melting, the permafrost degradation and the generation of extreme events like rapid and severe rainstorms. All these aspects have contributed to increase the possibility of occurrence of a particular type of landslide: debris flows (Zimmerman and Haerberli 1992).

Debris flow is a paroxystic phenomenon due to a rapid or extremely rapid mobilization of a mixture of water, sediments and floating material into a steep channel (Iverson 1997; Hungr 2005). Their high density, greater than 1700 kg/m^3 (ONR-24800 2009) and high runout velocity, up to 20 m/s (Hungr et al. 2014) make them decisive in the morphological evolution of mountain areas, often extensively urbanized and therefore characterized by high hazard degree (Fioraso 2000). Their worldwide diffusion and the colonization of virgin areas, joined with the world population increase, grow up the probability for debris flow to cause disasters.

Like avalanches, debris flows occur with little warning and exert great loads on obstacles they encounter. Like water floods, they are fluid enough to travel long distances in channels and inundate vast areas (Iverson 1997). Moreover, their unpredictability hampers collection of detailed real event data.

Since risks cannot be eliminated but only mitigated, many mitigation strategies have been developed in the last years. When a potential source area is identified, since stabilization is not always a practical option, the consequences of failure must be considered. The latter are the basis for the design of mitigation measures and for the management of the residual risk (Jakob et al. 2016).

Mitigation measures can be divided in two different types:

- Active measures, which are focused on the hazard and essentially they prevent the debris flow triggering, transport and deposition and can therefore change debris magnitude and frequency characteristics (Huebl and Steinwendtner 2000; Kienholz 2003).
- Passive measures, which are focused on the potential damage and are used to change the vulnerability of debris flow either with hazard mapping (Bankoff et al. 2004; Griswold 2004) or through immediate disaster response (Kienholz 2003; Badoux et al. 2009; Santi et al. 2010).

Although passive measures are more advisable than active ones, the latter are necessary in order to correctly manage residual risk (Jakob and Hungr 2005). A correct land-use planning and a hazard management implicate lower costs (economical and social) but usually active measures are required, especially where there was an inadequate risk management.

Since protection structures are designed to withstand the impact force of the moving mass, the estimation of the potential impact pressure becomes a key aspect for safely design these mitigation measures. The scientific community has widely faced the challenge of debris flow hazard assessment, but universally recognized models for the design of these structures are still missing (Vagnon et al. 2016).

Data availability and universal applicability are the main issues for the development of predicting impact models. The lack of data from monitoring of debris flow events forces to perform small-scale (e.g. Armanini and Scotton 1992; Huebl and Holzinger 2003; Canelli et al. 2012; Wendeler and Volkwein 2015; Ashwood and Hungr 2016; Vagnon and Segalini 2016) and full-scale flume experiments (DeNatale et al. 1999; Bugnion et al. 2012). Laboratory tests are useful but they are affected by scale effects that cannot be properly quantified and, consequently, they may not replicate or be comparable with field data (Iverson 1997; Huebl et al. 2009). Thus, their results must be interpreted with a healthy dose of scepticism (Iverson 2015) since performing analogue experiments of large scale phenomena require satisfy all the relevant similarity criteria but this is impossible for debris flows (Turnbull et al. 2015). Researchers have to choose if maintain stress similarity or lost information on particle effects. The first scenario requires increasing the effective

gravity and consequently, performing centrifuge experiments. The use of uniform material, as in chute experiments, is a huge simplification because produces limited pore-fluid pressure effects and excessive pore-fluid shear resistances that can lead to underestimation of solid-fluid drag and dynamic effects. Consequently, an appropriate scale analysis is always required for the study of mass movements such as debris flows.

In 1996, the US Geological Surveys (DeNatale et al. 1999) performed debris flow impact text on flexible barriers in a full-scale concrete flume, highlighting that the inherent variability of a well-controlled, staged debris flow made it difficult to isolate the effect of any single parameter. Instead, Bugnion et al. (2011) in their full-scale experiments of hillslope debris flows, stated that pressures depend primarily on the flow speed, which in turn appears to depend on the grain-size distribution and water content.

As a consequence, even if the results of full- and small- texts are comparable to those observed in real-scale measurements and simulate quite well the physics of idealised debris flows, they may not describe well the rheology, the complex topography and the presence of obstacles (buildings, infrastructures etc.) along the debris flow path (Gao et al. 2017).

Many of these formulations yield a rough estimation of the debris flow impact pressure against structures due to their empirical nature, their validation only based on small-scale observations that could lead to high discrepancies with field observations (e.g. Hungr et al. 1984; Revellino et al. 2004; Zanchetta et al. 2004; Shen et al. 2018). Then, dimensions, types and inertial resistance of the barriers are completely neglected in most of these models (Vagnon and Segalini 2016).

Finally, for what it concerns the model validation, it is performed on limited datasets, both in terms of number and type of observations.

The aim of this paper is to analyse debris flow impact models proposed in scientific literature and evaluate the discrepancies between measured and numerically predicted results using ten datasets available in scientific literature. Sixteen formulations were accurately discussed, highlighting their strong points and their shortcomings. As a result of the data analysis, a new formulation is here presented.

The insights carried out from this paper will be useful for engineers to design debris flow protection measures. Moreover, the presented results will help engineers in the choice of the best debris flow impact model as a function of phenomenon features and mitigation measures technical characteristics.

The present study is organized into six sections: the first one is introductory and presents the most common mitigation methods for debris flows. The second section provides a review of debris flow impact models. Section three summarizes current international standards in debris-flow mitigation design. In section four and five, the impact models are compared and statistically analysed for evaluating their reliability in predicting measured pressure. Finally, an empirical model is proposed and the main results of this study are summarised and discussed.

DEBRIS FLOW CONTROL BY BARRIERS

The use of mitigation measures depends on the adopted protection strategy and on the objectives established from the risk assessment (Huebl 2001). The choice of the best mitigation measure must be evaluated with respect to its technical, economical, ecological and political feasibility.

Generally, the areas susceptible to debris flow phenomena are narrow and not suitable for installing large structures. Although setting only one structure is often by no means sufficient to make debris flow harmless and, moreover an integration of both active and passive measures should be encouraged (Takahashi 2007), in the last three decades many active mitigation measures have been installed worldwide. Active debris flow mitigation measures affect the initiation

or the transport or the deposition of debris flows. Mitigation measures have a direct effect on the magnitude and on the frequency of the phenomenon, changing the probability of the event or manipulating the debris flow itself. They must be designed to resist the impact force and their main tasks are: i) dissipate the debris flow kinetic energy and ii) retain totally or partially the debris flow material (VanDine 1996; Mizuyama 2008; Brighenti et al. 2013; Song et al. 2017; Wendeler et al. 2018).

Common debris flow structural measures include close-type check dams (Fig. 1a), open-type sabo dams (Fig. 1b), concrete slit sabo dams (Fig. 1c) and flexible net barriers (Fig. 1d).

Fig. 1 Different types of debris flow active mitigation measures: check dam (photograph by Los Angeles County Flood Control District) (a), open type Sabo structures (photograph of steel check dam in Nagano prefecture, Japan) (b), concrete slit barrier (photograph by LCW Consult web site of protection works in St. Luzia River, Madeira, Portugal) (c) and flexible net barrier (photograph by Geovertical S.R.L web site of protection works in Terranova Pollino, Basilicata Region, Italy) (d)

The design of these structures should comply with two requirements: firstly, it should take into account geographical, geological and site conditions. Secondly, at the end of design process the structural resistances shall be always greater than the effects of the forces exerted on the structure. For what it concerns the barrier resistance, it can be easily evaluated since the resistance of each single component is well known and accurately calculated. By contrast, the definition of the impacting load on the structure is an open issue (Vagnon et al. 2017a): as it will be described in the next section, there are many models for quantifying the stress distribution on the barrier, but none of them is universally recognized. Moreover, their predicting capability, that is an evaluation of the discrepancy between measured and estimated impact forces, especially using data collected from real events, is unknown. In particular, for mitigation measure designers become of utter importance to know under which dynamic features the impact models lead to an underestimation or excessive overestimation of the lad conditions.

Finally, it is important to underline that the accuracy of dimensioning procedure is therefore highly dependent on the quality of process scenario. Inaccurate assumptions may result in inefficient design or in a partial or total failure of the structure and can lead to negative consequences for the vulnerable area. This means that poor quality input data (flow velocity, thickness, density, volume etc.) arises uncertainties in the evaluation of impacting load.

DEBRIS FLOW IMPACT MODELS

For an efficient design of mitigation structures, the debris flow impact pressure exerted on barriers is of utter importance because it is the main factor that causes structural collapse (Hungr et al. 1984; Armanini 1997; Huebl et al. 2009; Ferrero et al. 2015). Furthermore, there is an increasingly greater need in predicting impact load for the assessment and the management of risk.

Debris flow involves fundamentally independent physical and dynamical processes that couldn't be controlled by one or two parameters. The flow is heterogeneous and the mixture density evolves strongly as a function of time and space due to mixing, phase separation and particle sorting: this aspect leads to drastic change of the local material composition and it can result in huge impact pressure differences during impact (Iverson 1997). Moreover, density, velocity and flow height should be considered as field variable due to their variation through space, along the channel path, and time, during the flow process (Hungr et al. 1984; Kwan 2012). For all these reasons, the development of a reliable debris flow impact scheme results extremely complex.

The design of mitigation structures should require simplified models to predict impact pressure with high reliability; these models should be universally recognized and should include few parameters, related to material and flow characteristics easy to estimate.

Finally, the modelling of debris flow surges is difficult because the impact pressure depends on a dynamic component exerted by the heterogeneous flow, that can reach 10 - $5x10^3$ kN m^{-2}, and an impulsive component generated by the single impact of boulders: the latter can vary between 10^2 and 10^4 kN m^{-2} (Suwa and Okuda 1983; Zhang 1993).

Moreover, the flow composition and the impact mechanism strongly influenced the impact load and its distribution on structures (Song et al. 2017). Many studies (Choi et al. 2015; Sovilla et al. 2016; Ng et al. 2019) on this topic have highlighted that when dry granular flows impacting a rigid barrier, a pileup mechanism developed. On the contrary, viscous flows exhibited the formation of a vertical-jet mechanism upon impact. This happens when the flow inertia is larger than restoring gravitational field (Poudyal et al. 2019). In fact, in viscous flow, the effect of particle shearing in kinetic energy dissipation is less significant compared to frictional-grain stresses in dry granular flow.

It is obvious that debris flow modelling requires many assumptions for simplifying its real complex nature: a) the mixture has to be considered as an equivalent fluid with averaged characteristics of density, b) the simultaneous occurrence of maximum velocity and thickness values, c) the rigid behaviour of the flow at the impact (Osanai et al. 2010; Suda et al. 2010; Kwan 2012).

On the basis of these hypotheses, in the last decades many methods were developed and, in general, they can be classified into hydraulic and solid-collision (Huebl et al. 2009) and shock-wave propagating upstream models (Chou et al. 2012; Albaba et al. 2018).

Hydraulic models, derived from fluid momentum balance and Bernulli's equation, schematize the flowing mass as a homogeneous mean (characterized by an average density between fluid and solid component) and consider the load as a modified value of hydro-dynamic pressure or a multiple of the hydro-static load or a combination of both.

The maximum impact pressure considering hydro-static model can be evaluated using the following equation:

$$p_{peak} = k \cdot \rho_m \cdot g \cdot h_f \quad (1)$$

where p_{peak} is the maximum impact load in N m^{-2}, k is an empirical coefficient, ρ_m is the mean density of the debris impacting fluid in kg m^{-3}, g is gravity in m s^{-2} and h_f is the flow height in m. This model is based on a triangular load distribution and the load increase factor, k (e.g. Lichtenhahn 1973; Armanini 1997). The latter can assume values ranging from 2.5 to 7.5.

Lichtenhahn (1973) firstly applied this equation for the evaluation of debris flow impact on concrete barrier, proposing k values between 3.5 and 5.5. Later, following the same theoretical principles of the previous study and comparing results with experimental tests, Armanini (1997) evaluated k as 4.5 times the hydro-static pressure. At the same time, Scotton and Deganutti (1997), performing small scale laboratory tests and measuring impact pressure on vertical obstacle, estimated k varying between 2.5 and 7.5, depending on the viscosity of the interstitial fluid and flow hydraulic conductivity.

The popularity of these formulations is due to their simplicity and the few number of parameters involved: in fact they only require debris density and flow height and usually flow height is considered equal to channel depth. On the other hand, they do not take into account flow rheological properties and they are only applicable with small velocity values or rather with flatter terrain.

196 Concerning hydro-dynamic models, the impact on the structure has a constant load distribution and the general equation
197 is:
198
199 $$p_{peak} = \alpha \cdot \rho_m \cdot v_f^2 \quad (2)$$
200
201 where α is the dynamic coefficient and v_f is the flow velocity in ms^{-1}.
202 The parameter α include information about the flow type, the formation of vertical jet-like wave at the impact, the grain
203 size distribution and the barrier type (Canelli et al. 2012).
204 Watanabe and Ikeya (1981) firstly applied this model for the analysis of volcanic mudflow in Japan. They found that α
205 ranged between 2 and 4 as a function of the grain size distribution of the mixture.
206 The following equation is the Hungr et al.' equation (1984) and it is maybe the most famous hydro-dynamic
207 formulation used for evaluating debris flow impact pressure against obstacles:
208
209 $$p_{peak} = 1.5 \cdot \rho_m \cdot v_f^2 \cdot sin\beta \quad (3)$$
210
211 where β is the least angle between the face of the barrier and the flow direction.
212 The dynamic coefficient equals to 1.5 was defined after the back-analysis of data from monitoring of real debris flow
213 events occurred in British Columbia (Canada). This coefficient was included for considering the generation of a
214 stagnant wedge behind protection barriers.
215 Moreover, in scientific literature exists a wide range of proposed values for the dynamic coefficient: Daido (1993)
216 suggested values varying between 5 and 12, Zhang (1993) recommended a range between 3 and 5, Bugnion et al.
217 (2011) measured values from 0.4 to 0.8, Canelli et al. (2012) between 1.5 and 5.
218 The values listed above prove that the range of variation of dynamic coefficient (between 0.4 and 12) deeply conditions
219 the evaluation of peak pressure: consequently, from an engineering point of view, the design of protection barriers is
220 strongly influenced by the choice of one formulation respect to another, arising uncertainties in the reliable evaluation
221 of the probability of failure of the mitigation measure.
222 Huebl and Holzinger (2003) developed a modified hydro-dynamic formula introducing Froude number (F_r) to
223 normalised impact force and achieved a scale-independent relationship:
224
225 $$p_{peak} = 5 \cdot \rho_m \cdot v_f^{0.8} \cdot (g \cdot h_f)^{0.6} \quad (4)$$
226
227 Using small-scale flume experiments and 155 sets of data coming from other authors, Cui et al. (2015) estimated the
228 peak impact pressure as:
229
230 $$p_{peak} = 5.3 \cdot F_r^{-1.5} \cdot \rho_m \cdot v_f^2 \quad (5)$$
231
232 Combining Equation 1 and 2, many Authors hypothesized new relationships to estimate maximum impact pressure
233 against barrier. The general relation is:
234
235 $$p_{peak} = \rho_m \cdot g \cdot h_f + \rho_m \cdot v_f^2 \quad (6)$$
236

Cross (1967) firstly modified the equation for perfect fluid used for evaluating tsunami impact forces introducing static coefficient, k, and dynamic coefficient, α, respectively equal to 0.5 and 3 as follow:

$$p_{peak} = k \cdot \rho_m \cdot g \cdot h_f + \alpha \cdot \rho_m \cdot v_f^2 \quad (7)$$

Later, Arattano and Franzi (2003), analysing measured data in Moscardo Torrent (Italy), validated Equation 6.
Other studies were carried out hypothesizing the total reflection of a flow against a vertical wall and, imposing the dynamic equilibrium (Lamberti and Zanuttigh 2004). The relation is:

$$\mathrm{p_{peak}} = \mathrm{C_c} \cdot \frac{\left(1+\sqrt{2}\mathrm{F_r}\right)^2}{2} \cdot \rho_\mathrm{m} \cdot \mathrm{g} \cdot \mathrm{h_f} \quad (8)$$

where *Cc* is an empirical coefficient calibrated considering the vertical acceleration caused by the presence of fine particles and boulder equal to 1.5.
Another equation to evaluate the dynamic impact of a debris flow against a vertical wall is presented by Armanini et al. (2011):

$$\mathrm{p_{peak}} = \left(1 + \frac{1}{2} \cdot \mathrm{F_r^2}\right) \cdot \left(1 + \frac{\alpha \cdot \mathrm{F_r^2}}{1+\frac{1}{2}\mathrm{F_r^2}}\right) \cdot \rho_m \cdot g \cdot h_f \quad (9)$$

where α is a coefficient equal to 1.
Recently, Vagnon and Segalini (2016), performing several small scale flume tests, proposed a new model that takes into account either flow characteristics, material properties and barrier dimensions. The numerical expression is given as:

$$\mathrm{p_{peak}} = \left(\frac{1}{2}K_a(n^2-1)cos\theta + \alpha Fr^2 cos\beta - tan\varphi' \frac{n-1}{sin\theta} cos\beta cos\theta\right)\rho_m g h_f \quad (10)$$

where K_a is active lateral earth pressure coefficient derived from Rankine theory, θ is slope angle in deg, β is the angle between the barrier and the normal at channel bottom, measured in deg, φ is the debris friction angle in deg and n is the filling ratio, that is the ratio between the barrier height and the flow height. In this relation, dynamic coefficient, α, can vary between 0.5 and 1.2.
Solid-collision models are based on the Hertz contact theory as the following:

$$F_B = K_c n a^{1.5} \quad (11)$$

where $\mathrm{K_c}$ is the load reduction factor that depends on barrier stiffness (Hungr et al. 1984; Kwan 2012; Ng et al. 2016), n takes into account the radius of impacting boulder, its Poisson's ratio and the Young's modulus of the boulder itself and the barrier. The parameter a, depends on boulder mass and impact velocity. In scientific literature, many solid-collision models have been presented (Kwan 2012; Faug 2015; Ng et al. 2016; Song et al. 2017): their use is related to the ratio between boulder dimension and debris flow thickness. Ng et al (2016) highlighted that if this ratio is lower than 0.6, solid-collision contribution can be neglected and the impact of debris flow can be calculated using Equation 2 with α equals to 2.5.

For what it concerns shock-wave models, the impacting force is considered as a combination of inertial and depth-dependent forces associated with features of the incoming flow (Albaba et al. 2018). Although the shock-wave solution is obtained from the jump conditions of the mass and momentum balances, its predictions are in good agreement with experimental results (Chou et al. 2012). The main limitation of these methods is the high sensitivity of peak force to sampling length (that defines the sample dimension for averaging flow motion characteristics): in particular, Albaba et al. (2018) highlighted that only for slope angle greater than 42.5° and sampling length greater than 35 times the average particle diameter, the peak force is well predicted.

One further remark has to be made concerning the use of all the presented methods in numerical modelling: many numerical codes (Hutter et al. 1994; Brighenti et al. 2013; Albaba et al. 2015; Ashwood and Hungr 2016; Leonardi et al. 2016; Vagnon et al. 2017b; Wendeler et al. 2018) have been developed on the basis of hydro-static and hydro-dynamic simplified approach.

In this paper only hydraulic models has been treated and discussed, since not all the necessary parameters were available for evaluating the contribution of solid-collision and shock-wave models.

Table 1 summarizes general equations of all the previous models, highlighting the range of variation for static (k) and dynamic (α) coefficient. Moreover, Table 1 includes information about the texting procedure and how α and k coefficients were evaluated (cfr. columns three and four of Table 1). These coefficients depend on the type of mitigation measure considered and the characteristics of flow, in terms of grain size and viscosity. Mainly, they were calibrated performing small-scale tests on rigid (e.g. Armanini 1997; Scotton and Deganutti 1997; Kwan 2012) or flexible barriers (e.g. Canelli et al. 2015; Ashwood and Hungr 2016; Wendeler et al. 2018) and more rarely, they were evaluated as a result of full-scale test or real debris flows (Arattano and Franzi 2003; Bugnion et al. 2011).

Table 1 – Summary of analysed hydraulic model for evaluating peak debris impacting pressure on barriers.

INTERNATIONAL GUIDANCES FOR MITIGATION DESIGN: AN OVERVIEW

At present, there are few existing international technical guidelines about debris flow mitigation measures, one of which is undoubtedly the ONR series (ONR 24800 to ONR 24803) developed by the Austrian "Wildbach und Lawinenverbauung" office (WLV). The debris flow load models and the design, construction and life cycle assessment of protection works are arranged in these standards (Suda et al. 2010). In particular, ONR 24801 defines two models for calculating debris flow impact pressure: the first one, named as simple model, is based on Equation 1, assuming that h_f is equal to the barrier height and k ranges normally between 3 to 6. The second one, named as complex model, corresponds to Equation 4. In both cases, the standard specifies that flow parameters must be given by an expert for torrential control. Moreover, twelve stress combinations are defined depending on the functional type of mitigation structure in order to take into account uncertainties and provide adequate design of mitigation measure. At European level, ONR series are the only standards concerning debris flow mitigation structure design: recently, the European Organisation for Technical Assessment published the new European Assessment Document (EAD 340020-00-0106 2016) concerning the flexible kits for retaining debris flows and shallow landslides/open hill debris flows. This regulation defines the main components and the methods to assess the performance of the kit. These guidelines concern only the certification of barrier performances but no information on load distribution are given.

Other existing standards are the Japanese NILIM (National Institute for Land and Infrastructure Management) 904 and 905 (Osanai et al. 2010) that define the design characteristics of Sabo barriers. Compare to Austrian ONR series, these guidances are less specific (Moase 2017) since they suggest considering different combination of external forces (static

water pressure, sediment pressure and fluid forces of debris flow) without providing any formulations for their calculation.

One of the most comprehensive standard is that developed by Geotechnical Engineering Office (GEO) of Hong Kong. In particular, the GEO report 270 (Kwan 2012) presents guidelines on the design of debris-resisting barrier. For what it concerns impact model, the design guidance recommends that the design loading on barrier is based on multi-surge scenario and the total load is considered as the sum of dynamic impact and boulder impact (if the existence of boulders or large hard inclusions in the flow cannot be precluded). Boulder impact should be calculated using the simplified form of Equation 11 as following:

$$F = K_c 4000 v^{1.2} r^2 \quad (12)$$

where K_c is equal to 0.1, v is the boulder impact velocity normal to the barrier and r is the radius of boulder. Dynamic load should be calculated using Equation 2 with α equals to 2.5.

Analysing the previous standards, it is clear that there is not a universally recognized impact model: each guideline is based on local experience of use of debris resisting barriers.

EVALUATION OF THE PREDICTING CAPABILITY OF DEBRIS FLOW IMPACT MODELS

As stated above, the design of mitigation measures requires defining the load exerted by the flow on structures. The equations listed in Table 1 show that universally recognize model does not exist and thus it becomes fundamental for designers to know the capability of these models to fit experimental and field measurements. The choice of a model in relation to another mainly depends on: a) how accurately is the calculated pressure compared to the measured one; b) the limitations (if any) in the applicability of the model.

The predicting capability of the previous models was evaluated by comparing the predicted results with data coming from ten different datasets available in scientific literature. As listed in Table 2, their choice was made on the basis of availability of both dynamic information (thickness, velocity and density) and impact features (impact load) and for ensuring that the datasets covered different testing scenarios (soil type, water content, channel slope, magnitude) and different scale approaches. The datasets included values of flow velocity, thickness and impacting peak pressure collected from small scale tests performed in specifically created flumes (Scheidl et al. 2013; Cui et al. 2015; Ashwood and Hungr 2016; Vagnon and Segalini 2016), from full-scale debris flow (DeNatale et al. 1999; Bugnion et al. 2011) and from monitoring of recurrent debris flow in the Jiangjia Ravine basin in China (Hu et al. 2011; Hong et al. 2015) and Illgraben debris flow monitoring site in Switzerland (McArdell 2016; Wendeler et al. 2007).

Moreover, The choice of analysing both small-scale tests and field data was made to understand if the approach here presented could produce reliable results and to dispel any doubts on the result interpretation. The author is conscious that miniaturized tests are affected by scale effects and investigated materials are usually not satisfyingly representative of material involved in debris flow phenomena, but if a trend is recognized in both datasets, the analysis can be considered as a sign of a reliable approach.

In this paper, the data of peak impact pressure were normalized by those of hydro-static pressure as follows:

$$\tilde{p} = \frac{p_{peak_{measured}}}{\rho \cdot g \cdot h_f} \quad (13)$$

These values were plotted as a function of the Froude number, *Fr*, of the flow in order to achieve scale-invariant description. Froude number is defined as the square root of the ratio between kinetic and gravity force of the flow and it is useful for demarcating quasi static rate-independent from speed-squared force contributions (Faug 2015). An important remark has to be done for the evaluation of Fr values: a recent study published by Ng et al. (2019) highlighted that the choice of frontal velocity and maximum flow depth within the frontmost region of the flow is crucial for properly characterising the impact mechanism. In particular, an estimation of non-frontal Fr values may lead to an underestimation of impact pressure by a factor of two.

In general, laboratory and field data accordingly show the same range of variation of the normalized peak pressure; for what it concerns the Froude number, the range of variation related to laboratory tests is wider than the field one. As stated above, this discrepancy can be attributed to scale effects. However, the two dataset globally have the same trend for $\tilde{p}$ as function of *Fr*.

The normalized pressures, $\tilde{p}$, were compared to all the listed above predicting models, considering for each one the upper and the lower limit of the range of variability of empirical coefficients k and α. For the sake of simplicity and readability of figures, the models were pooled into three groups (hydro-static, hydro-dynamic and mixed models) and plotted separately for better highlighting limitations and strong points for each model.

In Fig. 2, the predicting capability of hydro-static models is evaluated: in general, these formulations underestimate the normalized peak pressure measured both in small- and full-scale tests (Fig.s 2a and 2b) and field data (Fig. 2c), regardless of the value of empirical coefficient k.

In general, from an engineering point of view, the fact that hydro-static models underestimate the debris flow impact pressure (with the exception of Scotton and Deganutti (1997) model with k = 7.5 for Fr lower than 3) points out an inadequacy for the design of protection structures.

Fig. 2 Comparison between normalized debris flow impact force and hydro-static predicting models as function of Froude number considering small- (a) and full-scale experiments (b) and field data (c).

For a deeper analysis, the ratio between the measured peak pressure and the estimated one was calculated and reported in Fig. 3 as function of Froude number for both small- (a, d) and full-scale (b, e) and field datasets (c, f). The upper (7.5) and the lower (2.5) limits of the k range of variation were chosen in order to define the suitability for predicting impact pressure of the hydro-static models.

The peak pressure ratio gives information about the discrepancy between predicted results using hydro-static methods and measured ones: if this ratio is lower than 1, the predicting value overestimates the measured one, vice-versa the peak pressure is underestimated. If this ratio is 1, there is a perfect correspondence (green continuous line in Fig. 3) between measured values and predicted one. From an engineering point of view, for providing safe results, predicting models should exhibit a ratio lower than unity, and in particular varying between 0.5 and 1, so that the impacting pressure is reasonably overestimated. This aspect will be better explained in the next section.

Analysing Fig. 3, hydro-static formula with k = 2.5 (that corresponds to the lower limit of Scotton and Deganutti (1997) equation) always underestimates the measured peak pressure (Fig.s 3a to 3c). On the contrary, Scotton and Deganutti (1997) equation considering k = 7.5 simulates well about the 55% of the field data (Fig. 3f). These two equations define the variability domain of the existing hydro-static formulations.

Analysing Fig. 2 and Fig. 3, there is an evident non-linear relation between estimated pressure and Froude number: the higher is *Fr* a, the higher is the distance between measured and estimated pressure value. Moreover, considering

Scotton and Deganutti (1997) formulation (with k = 7.5), it seems that the prediction capability of this model is high for Fr < 3; in this case the percentage of peak pressure ratio lower than 1 increases till 70%.

It becomes obvious that hydro-static models are suitable only for low Froude numbers (generally lower than 3, Huebl and Holzinger 2003; Cui et al. 2015), namely when the flow is characterized by low velocity and dynamic components are negligible (Huebl and Holzinger 2003) (cfr. Fig. 3).

In this study, starting from this observation, an attempt to take into account dynamic effects in hydro-static models will be presented and discussed.

Fig. 3 Relationship between measured peak pressure and calculated hydro-static peak pressure with k respectively equal to 2.5 (a to c) and 7.5 (d to f) as a function of the Froude number considering both small- (a, d) and full- scale (b, e) and field dataset (c, f). The green continuous line represents the perfect correspondence between measured values and estimated ones.

Concerning hydro-dynamic models, they have a good capability in predicting the peak impact pressure (Fig. 4) except for models with dynamic coefficient, α, lower than 1 (Bugnion et al. (2011), cfr. Fig.s 5a to 5c). The two key points are: a) verify if the predicting capability is influenced by flow regime; b) considering maximum dynamic coefficient value (α = 12 from Daido (1993)) the peak values are excessively overestimated. The latter point has a great impact on the design of mitigation measures, in particular on their construction costs (cfr. next section).

In Fig. 4a, for very low Froude values (Fr < 2), it seems that hydro-dynamic models are affected by of the influence of flow regime, characterized by low velocity and high impact thickness. In this case, only Daido (1993) equation reaches to satisfactorily predict peak pressure.

Fig. 4 Comparison between normalized debris flow impact force and hydro-dynamic predicting models as function of Froude number considering small- (a) and full-scale tests (b) as well as field data (c).

Focusing on Hungr et al. (1984) equation (continuous blue line in Fig. 4), which is certainly the most famous, in the 86% of cases it overestimates the measured peak pressure. This formulation has a high predicting capability for high Froude values, meanwhile for Froude equal or lower 2 it underestimates measured pressure (Fig.s 4a and 4c). In Fig. 5, this aspect is better clarified: observing the pressure ratio, it decreases when Froude number increases following an inverse power law. Except for Bugnion et al (2011) equation (Fig.s 5a to 5c) for which the pressure ratio is almost never lower than unity, in the other formulations this relationship is verified for Fr > 2. Daido (1993) formulation with α = 12 (Fig.s 5d to 5f) deserves a debate of its own: in fact it excessively overestimates the pressure values (except for Fr < 2, confirming the observation made above), reducing pressure ratio close to 0. This latter point will be better argued in next section.

Fig. 5 Relationship between measured peak pressure and calculated hydro-dynamic peak pressure with α respectively equal to 0.4 (a to c) and 12 (c to d) as a function of the Froude number considering both small- (a, d) and full-scale (b, e) and field dataset (c, f)

Summarizing, the analysis performed on small- and full-scale and field data has highlighted that pure hydro-static and pure hydro-dynamic models are not totally adequate to predict debris flow impact pressure on structures. In Froude

region lower than 3, where velocity are low and impacting thickness are high (cfr. Fig. 6) hydro-static formulations perform well; on the contrary, hydro-dynamic models underestimate pressure values since kinetic effect are not dominant (Huebl and Holzinger 2003, Cui et al. 2015; Faug 2015).

Fig. 6 Relationship between velocity (blue squares) and thickness (red diamonds) as function of Froude number for small-scale tests (a) and full-scale and field data (b). A negative correlation exists between velocity and thickness: when Froude number increases, velocity increases and consequently flow height decreases and vice-versa.

In the light of previous observations, mixed models are more suitable for predicting impact loads as clearly showed in Fig. 7 in which all data (both from small- and full-scale tests and field measurements) fall into the region defined by these formulations.

Fig. 7 Comparison between normalized debris flow impact force and mixed predicting models as function of Froude number considering small- (a) and full-scale test (b) as well as field data (c).

For evaluating the performance of each formulation, the peak pressure ratio was evaluated, as shown in Fig. 8. For readability of the figure, only field data were plotted. However, mixed models showed the same behaviour regardless the choice of dataset. Generally, despite their prediction capability is more suitable than hydro-static and hydro-dynamic formulations, not all mixed models can be universally usable in practise. For instance, Huebl and Holzinger (2003) and Cui et al. (2015) equations perform well for Froude values lower than 3 (Fig.s 8a and 8b). Arattano and Franzi (2003) formulation provides a good correspondence between field data and predicted ones: on the contrary, Cross (1967) equation excessively overestimates pressure peak values (providing a peak pressure ratio close to 0, cfr. Fig. 8c). Armanini et al. (2011) equation shows a neglecting dependence with Froude number, which causes, particularly for low values ($Fr<2$), an underestimation of the peak pressure (Fig. 8e). This dependence is not evident in the other models (Fig. 8c and 8f).

Fig. 8 Relationship between measured peak pressure and calculated peak pressure for different mixed models as a function of the Froude number considering field dataset (a to f).

A COMPREHENSIVE STATISTICAL ANALYSIS OF PREDICTING IMPACT MODEL

In this section, the predicting capability of debris flow impact models has been statistically analysed.

In Table 3, the results of the comparison between all the described models and small- and full-scale/field datasets are presented. The percentage is referred to the number of predicted values greater than measured ones. This condition occurs when the model overestimates the impacting peak pressure. If the percentage is high, the model has a good capability of overestimating measured peak pressure; on the contrary, if the percentage is low, the model is not suitable for predicting impact pressure. However, the percentage of overestimated peak pressure values is not sufficient for evaluating the reliability of a predicting model. From an engineering point of view the excessive overestimation shall be avoided as much as underestimation since it is related to mitigation measure construction costs. Thus, for each models was calculated the percentage of data that fall into four classes of peak pressure ratio, defined as follow:

- From 0 to 0.5 (orange class): it represents an excessive overestimation and consequently higher construction costs. If the predicting model shows a high percentage of data in this class, it should be discarded.
- From 0.5 to 0.7 (yellow class): if the predicting model shows a high percentage of data in this class, a careful analysis of cost benefit should be conducted when considering the suitability of the model.
- From 0.7 to 1 (green class): if the predicting model shows a high percentage of data in this class, it is extremely accurate in estimating impact pressure.
- From 1 to 1.3 (yellow class): taking into account the uncertainties related to parameter measurement, a careful analysis should be performed for choosing or discarding the model.
- Greater than 1.3 (red class): if the predicting model shows a high percentage of data in this class, it is not suitable for estimating debris flow impact pressure.

This classification gave indications about the level of overestimation/underestimation, which is important especially for defining the degree of safety of the mitigation measure and, indirectly, its construction costs.

Figures 9 to 11 add more information to Table 3 about predicting capability of analysed impact models: in general, all the hydro-static models (Fig. 9) are not suitable to describe debris flow impact behaviour since they has an high percentage (greater than 30%) of values that fall into red class, regardless the k-coefficient value. Hydro-dynamic formulations have a high propensity to excessively overestimate impact pressure when $\alpha>2$ (Fig.s 10d to 10h). Vice-versa, when dynamic coefficient is lower than unit (Fig.s 10a and 10b), these models are not suitable for predicting impact load. Hungr et al. (1984) and Canelli et al. (2012) models with $\alpha=1.5$ (Fig. 10c) seem to be a good compromise between overestimation and prediction capability. Except for Croos (1967) equation (Fig. 11a) that exhibits an excessive overestimation, mixed models prove their adequacy as predicting methods since they show high percentage of values that fall into green class. In particular, Arattano and Franzi (2003), Armanini et al. (2011) and Vagnon and Segalini (2016) models (Fig.s 11b, 11c and 11g) result the most suitable for predicting real debris flow impact on structures due to the high percentage of data that fall into green class (more than 40%).

Fig. 9 Predicting capability analysis of hydro-static models using field dataset.

Fig. 10 Predicting capability analysis of hydro-dynamic models using field dataset.

Fig. 11 Predicting capability analysis of mixed models using field dataset.

TOWARDS A GENERALISED IMPACT MODEL

As highlighted in previous Sections, hydro-static formulations can be used, with a reliable degree of safety, to predict impact pressure for flows with $Fr < 3$. Moreover, analysing Table 3 and Fig. 9, it is evident how the predicting capability of these methods is very low: considering the highest k value, less than 55% of the peak pressure values are overestimated. This aspect cannot be neglected by mitigation measure designers and consequently, it makes these formulation not completely suitable for the estimation of impact forces on structures.

In the light of these aspects, is it possible to revise hydro-static model, improving its capability to overestimate field data?

Fig. 12 shows that a power law governs the trend between peak pressure ratio and Froude number. In particular the relation is:

$$\frac{p_{peak\_measured}}{\rho \cdot g \cdot h_f} = a \cdot Fr^b \quad (14)$$

where *a* and *b* are respectively equal to 1.38 and 1.64.

Fig. 12 Relationship between field measurements of the peak pressure and calculated peak pressure using hydro-static formulation with k = 1 as a function of the Froude number of the flow

Starting from Equation 14 and taking into account that estimated values should overestimate measured ones, the following modified hydro-static equation is proposed:

$$p_{peak} = 1.5 \cdot a \cdot Fr^b \cdot \rho \cdot g \cdot h_f = k^* \cdot \rho \cdot g \cdot h_f \quad (15)$$

where *a* and *b* are respectively equal to 1.38 and 1.64 as derived from data interpolation (Fig. 12) and 1.5 is an increasing coefficient for overestimating the impact pressure. The choice of 1.5 is done in order to obtain an average peak pressure ratio of 0.8 (red line in Fig. 13) so that the estimated pressure is reasonably overestimated.
It has been observed that in 86% of cases this formulation overestimates field data; this percentage is comparable with that obtained using hydro-dynamic and mixed models. The statistical analysis of predicting capability is comparable with that of mixed model, with high percentage of values falling into yellow and green classes (Fig. 13b). Moreover, analysing Fig. 13a, the Froude dependence exhibited by classic hydro-static models (cfr. Fig. 2 and Fig. 3) is not present in this modified formulation. On average, the peak pressure ratio (as function of Fr) has a horizontal trend. Only in correspondence of Fr = 2, few estimated values underestimate measured ones; however this aspect also occurs in Fig. 2 and Fig. 3 for other hydro-static models.

Fig. 13 Relationship between peak pressure ratio for the modified hydro-static model as a function of the Froude number (a) and statistical evaluation of the predicting capability of the proposed model (b).

This new formulation, although it follows the same theoretical concepts of hydro-static models, has an empirical nature since its empirical coefficient results from the analysis of field data. Fig. 14 shows the comparison between the proposed equation and the impact models that, on the basis of the previous statistical analysis, have exhibited the best predicting capability. Moreover, Lamberti and Zanuttigh (2004) and Armanini et al. (2011) models have some similarities with the proposed. In fact, the three formulations have analogous trends of p˜ as function of Fr; in general, mixed hydro-static models overestimate field data, particularly with high Fr, compared to the proposed one. Moreover, the new formulation introduces (on the basis on the used field dataset) the concept of reasonable overestimation (the increasing value of 1.5 of Equation 15 has been chosen for obtaining peak pressure ratio equals to 0.8) that it is not taken into account by other formulations. Obviously, the empirical coefficient k* should be reviewed increasing field data in order to reach more robust statistical analyses.

Fig. 14 Comparison between the proposed model (black line) and others hydro-dynamic (Hungr et al. 1984 and Canelli et al. 2012) and mixed (Arattano and Franzi 2003, Huebl and Holzinger 2003, Lamberti and Zanuttigh 2004, Armanini et al. 2011, Cui et al. 2015 and Vagnon and Segalini 2016) models.

DISCUSSION AND CONCLUSIONS

In this paper, sixteen debris flow impact models have been described and their predicting capability, or better their capability to fit experimental and field data, has been evaluated using three different dataset: one coming from small-scale flume tests, one from full-scale experiments and one from real data collected at Jiangjia Ravine (China) and Illgraben (Switzerland) basins. At first sight, the small-scale dataset showed dimensionless pressure values shifted to higher Froude numbers compared to those obtained from on-site dataset. This difference is a consequence of the scale effects that affect the small-scale tests and probably due to the influence of the triggering mechanism.

This study is a first attempt to compare the most famous debris flow impact models, analysing their strong points and limitations and evaluating their capability of fitting experimental and field data for helping designers in the choice of the best models to design mitigation measures (Kwan 2012).

For the sake of simplicity and for a direct comparison between the described methods, the models have been classified into three groups: hydro-static, hydro-dynamic and mixed models. For each model, key points and limitations have been highlighted and the main findings can be summarized as follow:

1. Hydro-static models require few input parameters (flow density and thickness) for evaluating impact pressure on structures. This aspect is particularly important for what it concerns the level of uncertainties coming from the whole debris flow scenario: since these parameters can be easily evaluated analysing past events, the result variability depends mainly by the dimensionless coefficient k. By contrast, the performed analyses have shown that the predicting capability reached an acceptable level of safety for Froude number lower than 3. Moreover, the predicting capability decreases of about the square of the Froude number, confirming that when the velocity of the flow increases (and consequently the flow thickness decreases) these models are not able to predict impact load. The performed statistical analysis also confirmed the limited suitability of these models.
2. Hydro-dynamic models provide impact pressure considering the flow density and the square velocity of the flow. The latter parameter is particularly difficult to measure during debris flow event and for this reason the related uncertainties can result high. As highlighted above, except for those models with α lower than 1 (Bugnion et al., 2011), hydro-dynamic formulations have a good capability to predict and overestimate impact pressure especially for high Froude numbers (predicting capability is low when Fr is lower than 2). However, the main limitation is the excessive overestimation in predicting impact load that may results in a large increment of costs for structure construction. A dynamic coefficient equal to 2 is suggested, as a good compromise between predicting capability and excess of overestimation.
3. Mixed models seem to be best methods for predicting debris flow impact pressure on barriers, since they include both information about the static and the dynamic component of the flow. The increase in the numbers of parameters increases the uncertainties and, consequently, the degree of reliability of these methods decreases.

The main hypothesis behind the described methods is that the entire load is totally transferred to the structure, without any dissipation during the impact. In terms of barrier design, this hypothesis should lead to over-conservative design since stiffness and drainage capability are not taken into account. Analysing field results, the overestimation induced by this hypothesis is not always verified probably due to the hit of single boulders on the barrier, condition that required the introduction of specific equations (Kwan 2012; Faug 2015; Ng et al. 2016; Song et al. 2017) or the increase of the dimensionless coefficient (k and α).

Finally, the model proposed in this paper exhibits a good capability to predict impact load. It is able to take into account both the static and the dynamic behaviour of the flow without being affected by of the influence of flow regime. Further monitoring field data will be helpful eventually to review the statistics at the basis of this new formulation and to

602 improve its predicting capability. Moreover, additional monitoring debris flow systems would be very welcome to
603 improve the knowledge about these disastrous phenomena and help to design mitigation measures with increasing level
604 of safety and reliability.
605 It is expected that the results proposed in this paper will be useful for designer, helping them for the best choice of
606 debris flow impact models on barriers.

607 **References**

608 Albaba A, Lambert S, Nicot F, Chareyre B (2015) Relation between microstructure and loading applied by a granular
609 flow to a rigid wall using DEM modeling. Granular matter 17(5):603-616.
610
611 Albaba A, Lambert S, Faug T (2018) Dry granular avalanche impact force on a rigid wall: Analytic shock solution
612 versus discrete element simulations. Physical Review E 97:052903-1–12.
613
614 Arattano M, Franzi L (2003) On the evaluation of debris flows dynamics by means of mathematical models. Nat
615 Hazards Earth Syst Sci 3:539–544. doi:10.5194/nhess-3-539-2003.
616
617 Armanini A, Scotton P (1992) Experimental analysis on the dynamic impact of a debris flow on structures. In
618 Proceedings of the Internationl Symposium Interpraevent. Bern, Switzerland 107–116.
619
620 Armanini A (1997) On the dynamic impact of debris flows. Recent developments on debris flows. In: Armanini A. and
621 Michiue M. (eds) Lecture notes in Earth Sciences 208–224. Springer, Berlin.
622
623 Armanini A, Larcher M, Odorizzi M (2011) Dynamic impact of a debris flow front against a vertical wall. Ital J Eng
624 Geol Environ 1041–1049.
625
626 Ashwood W, Hungr O (2016) Estimating the total resisting force in a flexible barrier impacted by a granular avalanche
627 using physical and numerical modeling. Can Geotech J 53(10):1700-1717.
628
629 Badoux A, Graf C, Rhyner J, Kuntner R, McArdell BW (2009) A debris-flow alarm system for the Alpine Illgraben
630 catchment: design and performance. Nat Hazards 49:517–539.
631
632 Bankoff G, Frerks G, Hilhorst D (eds) (2004) Mapping vulnerability: disasters, development and people. Earthscan,
633 London
634
635 Brighenti R, Segalini A, Ferrero AM (2013) Debris flow hazard mitigation: a simplified analytical model for the design
636 of flexible barriers. Comp Geotech 54:1-15.
637
638 Bugnion L, McArdell BW, Bartelt P, Wendeler C (2011) Measurements of hillslope debris flow impact pressure on
639 obstacles. Landslides 9:179–187.
640
641 Canelli L, Ferrero AM, Migliazza M, Segalini A (2012) Debris flow risk mitigation by the means of rigid and flexible
642 barriers – experimental tests and impact analysis. Nat Hazards Earth Syst Sci 12:1693–1699. doi:10.5194/nhess-12-
643 1693-2012.
644
645 Choi CE, Au-Yeung SCH, Ng CWW (2015) Flume investigation of landslide granular debris and water run-up
646 mechanisms. Géotechnique Letters 5(1):28–32.
647

Chou SH, Lu LS, Hsiau SS (2012) DEM simulation of oblique shocks in gravity-driven granular flows with wedge obstacles. Granular Matter 14(6):719-732.

Cross RH (1967) Tsunami Surge Forces. Journal of the Waterways and Harbors Division, ASCE 93(4):201-231.

Cui P, Zheng C, Lei Y (2015) Experimental analysis on the impact force of viscous debris flow. Earth Surface Process and Landforms 40:1644–1655.

Daido A (1993) Impact force of mud debris flows on structures, Technical Session B. In Proceedings of the XXV IAHR Congress. Tokio, Japan 211–213.

DeNatale JS, Iverson RM, Major JJ, LaHusen RG, Fiegel GL, Duffy JD (1999) Experimental Testing of Flexible Barriers for Containment of Debris Flows. USGS Open File Report 38:99-205.

EAD 340020-00-0106 (2016) Flexible kits for retaining debris flows and shallow landslides/open hill debris flows.

Faug T (2015) Macroscopic force experienced by extended objects in granular flows over a very broad Froude-number range. Eur Phys J E 38(34):1-10.

Ferrero AM, Segalini A, Umili G (2015) Experimental tests for the application of an analytical model for flexible debris flow barrier design. Engineering Geology 185: 33-42.

Fioraso G (2000) Indagini geologico-morfologiche su aste torrentizie della valtellina e della Valle di Susa ricorrentemente soggette a colate detritiche torrentizie (debris flow). Quaderni di studi e documantazione 23, Supplemento GEAM 1:3-59 (in Italian)

Gao L, Zhang LM, Chen HX (2017) Two-dimensional simulation of debris flow impact pressures on buildings. Engineering Geology 226: 236-244.

Griswold JP (2004) Mobility statistics and hazard mapping for non-volcanic debris flows and rock avalanches. MS thesis, Portland State University

Hong Y, Wang JP, Li DQ et al. (2015) Statistical and probabilistic analyses of impact pressure and discharge of debris flow from 139 events during 1961 and 2000 at Jiangjia Ravine, China. Engineering Geology 187:122-134.

Hu K, Wei F, Li Y (2011) Real-time measurement and preliminary analysis of debris-flow impact force at Jiangjia Ravine, China. Earth Surface Processes and Landforms. 36:1268-1278.

Huebl J, Steinwendtner H (2000) Debris flow hazard assessment and risk mitigation. Felsbau, Rock and Soil Engineering, Vol.1, 17-23, Verlag Glueckauf (in German)

689 Huebl J (2001) Strategy of protection. In: R. Didier and F. Zanolini (eds), Risques torrentiels. Universitè Européenne
690 d'Eté sur les Risques Natureles, Grenoble, France.
691
692 Huebl J, Holzinger G (2003) Kleinmassstaebliche Modellversuche zur Wirkung von Murbrechern. WLS Report 50,
693 Institut fur Alpine Naturgefahren, Wien. 3 pp. (in German).
694
695 Huebl J, Suda J, Proske D et al. G (2009) Debris Flow Impact Estimation. In Proceedings of 11th International
696 Symposium on Water Management and Hydraulic Engineering (WMHE2009) Vol. 1:137-148.
697
698 Hungr O, Morgan GC, Kellerhals R (1984) Quantitative analysis of debris torrent hazard for design of remedial
699 measures. Can Geotech J 21:663–667.
700
701 Hungr O (2005) Classification and terminology. In: Debris flow Hazards and Related Phenomena. Edited by M. Jakob
702 and O. Hungr. Praxis Publishing Ltd., Chichester, UK 11-51.
703
704 Hungr O, Leroueil S, Picarelli L (2014) The Varnes classification of landslide types, an update. Landslides 11: 167-194.
705
706 Hutter K, Svendsen B, Rickenmann D (1994) Debris flow modeling: A review. Continuum mechanics and
707 thermodynamics 8(1):1-35.
708
709 Iverson RM (1997) The physics of debris flows. Rev Geophys 35:245–296.
710
711 Iverson RM (2015) Scaling and design of landslide and debris-flow experiments. Geomorphology 244:9-20.
712
713 Jakob M, Hungr O (2005) Debris-flow Hazards and Related Phenomena. Springer-Verlag Berlin Heidelberg 445-487.
714
715 Jakob M, Holm K, McDougall S (2016) Debris-flow risk assessment. Oxford Research Encyclopedias – Natural Hazard
716 Science. DOI: 10.1093/acrefore/9780199389407.013.37
717
718 Kienholz H (2003) Early warning systems related to mountain hazards. In: J. Zschau and A. Kueppers (eds), Early
719 Warning System for Natural Disaster Reduction: 3rd International IDNDR Conference on Early Warning System for the
720 Reduction of Natural Disasters. Postdam, 1998, 555-564, Springer-Verlag, Berlin.
721
722 Lamberti A, Zanuttigh B (2004) Experimental analysis of the impact of dry granular debris flows against obstacles.
723 XXIX Convegno di idraulica e costruzioni idrauliche, Trento 571–578.
724
725 Leonardi A, Wittel FK, Mendoza M, Vetter R, Herrmann HJ (2016) Particle–fluid–structure interaction for debris flow
726 impact on flexible barriers. Computer-Aided Civil and Infrastructure Engineering 31(5):323-333.
727
728 Lichtenhahn C (1973) Die Berechnung von Sperren in Beton und Eisen- beton, Kolloquium on Torrent Dams, Heft,
729 Mitteilungender Forstlichen Bundensanstalt Wien. 91–127. (in German)

730
731 Mizuyama T (2008) Structural countermeasures for debris flow disasters. International Journal of Erosion Control
732 Engineering 1(2):38-43.
733
734 Moase EE (2017) Guidance for debris-flow and debris-flood mitigation design. Simon Fraser University. Master Thesis
735
736 Ng CWW, Song D, Choi CE, Koo CH, Kwan JSH (2016) A novel flexible barrier for landslide impact in centrifuge.
737 Géotechnique Lett 6(3):221-225.
738
739 Ng CWW, Choi CE, Goodwin GR (2019) Froude characterization for single-surge unsteady dry granular flows: impact
740 pressure and run up. Can Geotech J DOI: 10.1139/cgj-2018-0529.
741
742 Osanai N, Mizuno H, Mizuyama T (2010) Design Standard of Control Structures Against Debris Flow in Japan. Journal
743 of Disaster Research 3(5):307-314.
744
745 Poudyal S, Choi CE, Song D et al. (2019) Review of mechanisms of debris-flow impact against barriers. In Proceeding
746 of the 7th International Conference on Debris-Flow Hazards Mitigations, Colorado, USA 1027-1034.
747
748 Revellino P, Hungr O, Guadagno FM, Evans SG (2004) Velocity and runout simulation of destructive debris flows and
749 debris avalanches in pyroclastic deposit, Campania region, Italy. Environmental Geology 45:295-311.
750
751 Santi PM, Hewitt K, VanDine DF, Barillas Cruz E (2011) Debris-flow impact, vulnerability, and response. Nat Hazards
752 56(1): 371-402. DOI: 10.1007/s11069-010-9576-8
753
754 Scheidl C, Chiari M, Kaitna R, Mulleger M, Krawtschunk A, Zimmerman T, Proske D (2013) Analysing Debris Flow
755 Impact Models, Based on a Small Scale Modelling Approach. Surv Geophys 34:121-140.
756
757 Scotton P, Deganutti AM (1997) Phreatic line and dynamic impact in laboratory debris flow experiments. In
758 Proceedings of the 1st ASCE International Conference on Debris-flow Hazard Mitigation: Mechanics, Prediction and
759 Assessment. San Francisco, USA 777–786.
760
761 Shen W, Zhao T, Zhao J, Dai F, Zhou G (2018) Quantifying the impact of dry debris flow against a rigid barrier by
762 DEM analyses. Engineering Geology 241:86-96.
763
764 Song D, Choi CE, Ng CWW, Zhou GGD (2017) Geophysical flows impacting a flexible barrier: effects of solid-fluid
765 Interaction. Landslides 15(1):99-110.
766
767 Sovilla B, Faug T, Kohler A, Baroudi D, Fischer J, Thibert E (2016) Gravitational wet avalanche pressure on pylon-like
768 structures. Cold Regions Science and Technology 126:66–75.
769

770 Suda J, Huebl J, Bergmeister K (2010) Design and construction of high stressed concrete structures as protection works
771 for torrent control in the Austrian Alps. In Proceedings of 3rd fib international Congress, Washington, USA, 1-12.
772
773 Suwa H, Okuda S (1983) Deposition of debris flows on a fan surface, Mt. Yakedake, Japan. Zeitschrift Geomorph N F
774 Suppl Bd 46:79–101.
775
776 Takahashi T (2007) Debris Flow. Mechanics, Prediction and Countermeasures. Taylor and Francis Group.
777
778 Turnbull B, Bowman ET, McElwaine JN (2015) Debris flow: experiments and modelling. Comptes rendus physique
779 16:86-96.
780
781 Vagnon F, Ferrero AM, Segalini A (2016) EC7 design approach for debris flow flexible barriers: applicability and
782 limitations. In: Gercek H., Ulusay R., Hindistan M.A., Tuncay E., Aydan O. (eds), Mechanics and Rock Engineering:
783 From the Past to the Future. International Symposium on International Society for Rock Mechanics, ISRM 2016.
784 Cappadocia, Turkey, 29-31 August 2016, 1, 499-504, CRC Press/Balkema.
785
786 Vagnon F, Segalini A (2016) Debris flow impact estimation on a rigid barrier. Nat Hazards Earth Syst Sci 16:1691–
787 1697. doi:10.5194/nhess-16-1691-2016.
788
789 Vagnon F, Ferrero AM, Umili G, Segalini A (2017a) A Factor Strength Approach for the Design of Rock Fall and
790 Debris Flow Barriers. Geotech Geol Eng 35(6):2663-2675.
791
792 Vagnon F, Ferrero AM, Latham JP, Xiang J (2017b) Benchmarking of debris flow experimental tests using combined
793 finite-discrete element method, FEMDEM. In Proceedings of ISRM Afrirock – Rock Mechanics for Africa, 739-752.
794
795 VanDine DF (1996) Debris flow control structures for forest engineering. Research Branch, BC Ministry of Forests,
796 Victoria, BC. Working paper 08/1996. 75 pages.
797
798 Watanabe M, Ikeya H (1981) Investigation and analysis of volcanic mud flows on Mount Sakurajima, Japan. Erosion
799 sediment transport measurement. In: Int Assoc Hydrol Sei Publ, 133, Florence, 245–256.
800
801 Wendeler C, Volkwein A (2015) Laboratory tests for the optimization of mesh size for flexible debris-flow barriers, Nat
802 Hazards Earth Syst Sci 15:2597-2604. DOI:10.5194/nhess-15-2597-2015.
803
804 Wendeler C, Volkwein A, McArdell BW, Bartelt P (2018) Load model for designing flexible steel barriers for debris
805 flow mitigation. Canadian Geotechnical Journal 99:1-39.
806
807 Zanchetta G, Sulpizio R, Pareschi M, Leoni F, Santacroce R (2004) Characteristics of May 5-6, 1998 volcaniclastic
808 debris flows in the Sarno area (Campania, southern Italy): Relationships to structural damage and hazard zonation.
809 Journal of volcanology and geothermal research 133:377-393.
810

811 Zhang S (1993) A comprehensive approach to the observation and prevention of debris flows in China. Nat Hazards
812 7:1–23.
813
814 Zimmerman M, Haeberli W (1992) Climatic change and debris flow activity in high mountains areas. A case study in
815 the Swiss Alps. Catena Suppl 22:59–72.
816

817 **List of Figures**

818 **Fig. 1** Different types of debris flow active mitigation measures: check dam (photograph by Los Angeles County Flood
819 Control Distric) (a), open type sabo structures (photograph of steel check dam in Nagano prefecture, Japan) (b),
820 concrete slit barrier (photograph by LCW Consult web site of protection works in St. Luzia River, Madeira, Portugal)
821 (c) and flexible net barrier (photograph by Geovertical S.R.L web site of protection works in Terranova Pollino,
822 Basilicata Region, Italy) (d).
823

824 **Fig. 2** Comparison between normalized debris flow impact force and hydro-static predicting models as function of
825 Froude number considering small- (a) and full-scale experiments (b) and field data (c).
826

827 **Fig. 3** Relationship between measured peak pressure and calculated hydro-static peak pressure with k respectively equal
828 to 2.5 (a to c) and 7.5 (d to f) as a function of the Froude number considering both small- (a, d) and full- scale (b, e) and
829 field dataset (c, f). The green continuous line represents the perfect correspondence between measured values and
830 estimated ones.
831

832 **Fig. 4** Comparison between normalized debris flow impact force and hydro-dynamic predicting models as function of
833 Froude number considering small- (a) and full-scale tests (b) as well as field data (c).
834

835 **Fig. 5** Relationship between measured peak pressure and calculated hydro-dynamic peak pressure with α respectively
836 equal to 0.4 (a to c) and 12 (c to d) as a function of the Froude number considering both small- (a, d) and full-scale (b,
837 e) and field dataset (c, f)..
838

839 **Fig. 6** Relationship between velocity (blue squares) and thickness (red diamonds) as function of Froude number for
840 small-scale tests (a) and full-scale and field data (b). A negative correlation exists between velocity and thickness: when
841 Froude number increases, velocity increases and consequently flow height decreases and vice-versa.
842

843 **Fig. 7** Comparison between normalized debris flow impact force and mixed predicting models as function of Froude
844 number considering small- (a) and full-scale test (b) as well as field data (c).
845

846 **Fig. 8** Relationship between measured peak pressure and calculated peak pressure for different mixed models as a
847 function of the Froude number considering field dataset (a to f).
848

849 **Fig. 9** Predicting capability analysis of hydro-static models using field dataset.
850

851 **Fig. 10** Predicting capability analysis of hydro-dynamic models using field dataset.
852

853 **Fig. 11** Predicting capability analysis of mixed models using field dataset.
854

855 **Fig. 12** Relationship between field measurements of the peak pressure and calculated peak pressure using hydro-static
856 formulation with k=1 as a function of the Froude number of the flow
857

858 **Fig. 13** Relationship between peak pressure ratio for the modified hydro-static model as a function of the Froude
859 number (a) and statistical evaluation of the predicting capability of the proposed model (b).
860
861 **Fig. 14** Comparison between the proposed model (black line) and others hydro-dynamic (Hungr et al. 1984 and Canelli
862 et al. 2012) and mixed (Arattano and Franzi 2003, Huebl and Holzinger 2003, Lamberti and Zanuttigh 2004, Armanini
863 et al. 2011, Cui et al. 2015 and Vagnon and Segalini 2016) models.
864

865 **List of Tables**

866 **Table 1 – Summary of hydraulic model for evaluating peak debris impacting pressure on barriers.**

Author	Coefficient	Data source	Notes
Lichtenhahn (1973)	3.5 – 5.5	Theoretical and construction experience	Hydro-static formula
Armanini (1997)	4.5	Theoretical and laboratory experiments	Hydro-static formula
Scotton and Deganutti (1997)	2.5 – 7.5	Laboratory experiments	Hydro-static formula
Watanabe and Ikeya (1981)	2.0 – 4.0	Field measurements of volcanic mud flows	Hydro-dynamic model
Daido (1993)	5 – 12	Analytical results	Hydro-dynamic model
Bugnion et al. (2011)	0.4 – 0.8	Measurements of generated hillslope debris flow at Canton Aargau, Switzerland	Hydro-dynamic model
Canelli et al. (2012)	1.5 – 5.5	Laboratory experiments and field measurements	Hydro-dynamic model
Hungr et al. (1984)	1.5	Back-analysis data in British Columbia, Canada	Hydro-dynamic model
Zhang (1993)	3.0 – 5.0	Field measured data in Jiangjia ravine, China	Hydro-dynamic model
Huebl and Holzinger (2003)	5	Field and laboratory experimental data	Mixed model
Cui et al. (2015)	5.3	Field and laboratory experimental data	Mixed model
Cross (1967)	$k = 0.5$ $\alpha = 3$	Tsunami wave pressure	Mixed model
Arattano and Franzi (2003)	1	Field measured data in Moscardo Torrent, Italy	Mixed model
Lamberti and Zanuttigh (2004)	1.5	Theoretical and laboratory experiments	Mixed model
Armanini et al. (2011)	1	Theoretical and laboratory experiments	Mixed model
Vagnon and Segalini (2016)	0.5 – 1.2	Theoretical and laboratory experiments	Mixed model

867

868 **Table 2 – Summary of the main dataset characteristics.**

	Dataset	Apparatus/Basin	Material	Measured Physical Quantities	Dimension of the dataset
Small-scale experiments	Scheidl et al. 2013	Wood flume with constant inclination of 30° and measuring section 4.5 m long and 0.45 m wide. The reservoir section can release a volume equals to 0.33 m3 of mixture.	Mixture with constant dry mass and variable water content (from 0.16 to 0.27). The grain size distrubution ranges between 0.0002 and 50 mm	Flow velocity, impacting height and horizontal impact forces recorded in real time during the experiments.	30 experiments but only 16 selected for further analyses
	Cui et al. 2015	Steel flume 0.2 m wide and 3 m long with slope ranging from 10° to 15°.	Material collected in the Jiangjia Ravine basin (China) with grain size distrubution varying between 0.001 and 10 mm. The liquid concentration varies from 0.34 to 0.76.	Flow velocity, impacting height and pressure recorded in real time during the experiments.	27 tests with different density (1600-2300 kg m-3) and slopes (10-13°).
	Ashwood and Hungr 2016	Steel flume 0.3 m wide and 3 m long with slope ranging from 22° to 34°.	Uniform quartz sand and pea gravel	Flow velocity, impacting height, profile, barrier deflection and pressure recorded in real time during the experiments.	28 tests with different density (1560-1780 kg m-3) and slopes (122-34°).
	Vagnon and Segalini 2016	Steel flume 4 m long and 0.39 m wide in which the slope is variable between 30° and 35°	Saturated sand with constant liquid concentration (0.4) and mixture density (1920 kg m-3). The grain size distribution varies between 0.0001 and 5 mm.	Flow velocity, impacting height and impact forces recorded in real time during the experiments.	63 test with different volume released and different slopes.
Full-scale experiments	DeNatale et al. 1999	A 41m long, 8m wide channel constructed on the side of a rock quarry near Velthein, Switzerland. Average inclination of 30°	Mixture of soil, bedrock and water	Flow height at the middle of channel, velocity of upper flow surface, impact pressure on two different steel plates	16 tests with single or multiple releases. Density varies between 1760 and 2110 kg/m3
	Bugnion et al. 2011	USGS debris flow flume, 95m long, 2m wide and 1.2 deep, with constant slope of 31°	Poorly graded, clean and saturated gravelly sand	Flow height, velocity, impact pressure on flexible barrier	6 experiments on flexible barriers
Field measurements	Wendeler et al. 2007	Barrier system installed at the Illgraben basin, Switzerland	Muddy debris flow	Flow height, load cells, velocity from video record	May 18th 2006 event
	Hu et al. 2011	Jiangjia Ravine basin, located near the city of Dongchuan (China). the basin has an area of 48.6 km2 and the mainstream has a length of 13.9 km.	The bulk density ranges from 1600 to 2300 kgm-3 with fluid concentration ranging from 0.15 to 0.6. The dimension of the solid particles varies between 0.001 and	Flow velocity, impacting height and impact forces recorded in real time during debris flow events.	38 surges occurede on August 25, 2004 after short intence rainfall

		100 mm.		
Hong et al. 2015	Jiangjia Ravine basin, located near the city of Dongchuan (China). the basin has an area of 48.6 km2 and the mainstream has a length of 13.9 km.	The bulk density ranges from 1600 to 2300 kgm-3 with fluid concentration ranging from 0.15 to 0.6. The dimension of the solid particles varies between 0.001 and 100 mm.	Channel width, flow velocity, impacting height, density, duration and impact forces recorded in real time during debris flow events.	139 events during 1961 and 2000
McArdell 2016	Illgraben basin, Switzerland	Quarzite and dolomite boulders, clat-size particles	Flow height, load cells, velocity from video record	29 July, 8 August and 24 August 2013 events

869

870 **Table 3 – Evaluation of the peak pressure prediction capability for debris flow impact models.**

Model type	Equation	Empirical coefficient [-]	Percentage of overestimated peak pressure values [%]		
			Small-scale dataset	Full-scale dataset	Field measurement
Hydro-static models	Lichtenhan (1973)	3.5	14.2	8.3	14.6
		5.5	17.2	12.5	35.6
	Armanini (1993)	4.5	15.7	8.3	25.4
	Scotton and Deganutti (1997)	2.5	11.2	8.3	5.4
		7.5	20.9	33.3	54.7
Hydro-dynamic models	Watanabe and Ike (1981)	2	82.1	100	91.2
		4	91	100	97.6
	Hungr et al. (1984)	1.5	72.4	91.7	86.1
	Daido (1992)	5	93.3	100	99
		12	100	100	98.7
	Zang (1993)	3	88.1	100	95.3
		5	93.3	100	99
	Bugnion et al. (2011)	0.4	0	4.2	2
		0.8	34.33	66.7	16.9
	Canelli et al. (2012)	1.5	72.4	91.7	86.1
		5.5	93.3	100	99
Mixed models	Cross (1967)	$k = 1; \alpha = 3$	88.1	100	94.3
	Arattano and Franzi (2003)	1	48.5	83.3	66.8
	Huebl and Holzinger (2003)		38.1	79.2	80.9
	Lamberti and Zanuttigh (2004)		64.2	100	87.9
	Armanini et al. (2011)	1	70.1	91.7	76.8
	Cui et al. (2015)		20.9	54.2	65.4
	Vagnon and Segalini (2016)	1.2	85.1	87.5	84.6
Number of small-scale tests			134		
Number of small-scale tests			24		
Number of field measurements			298		

871

872

873 **Figures**

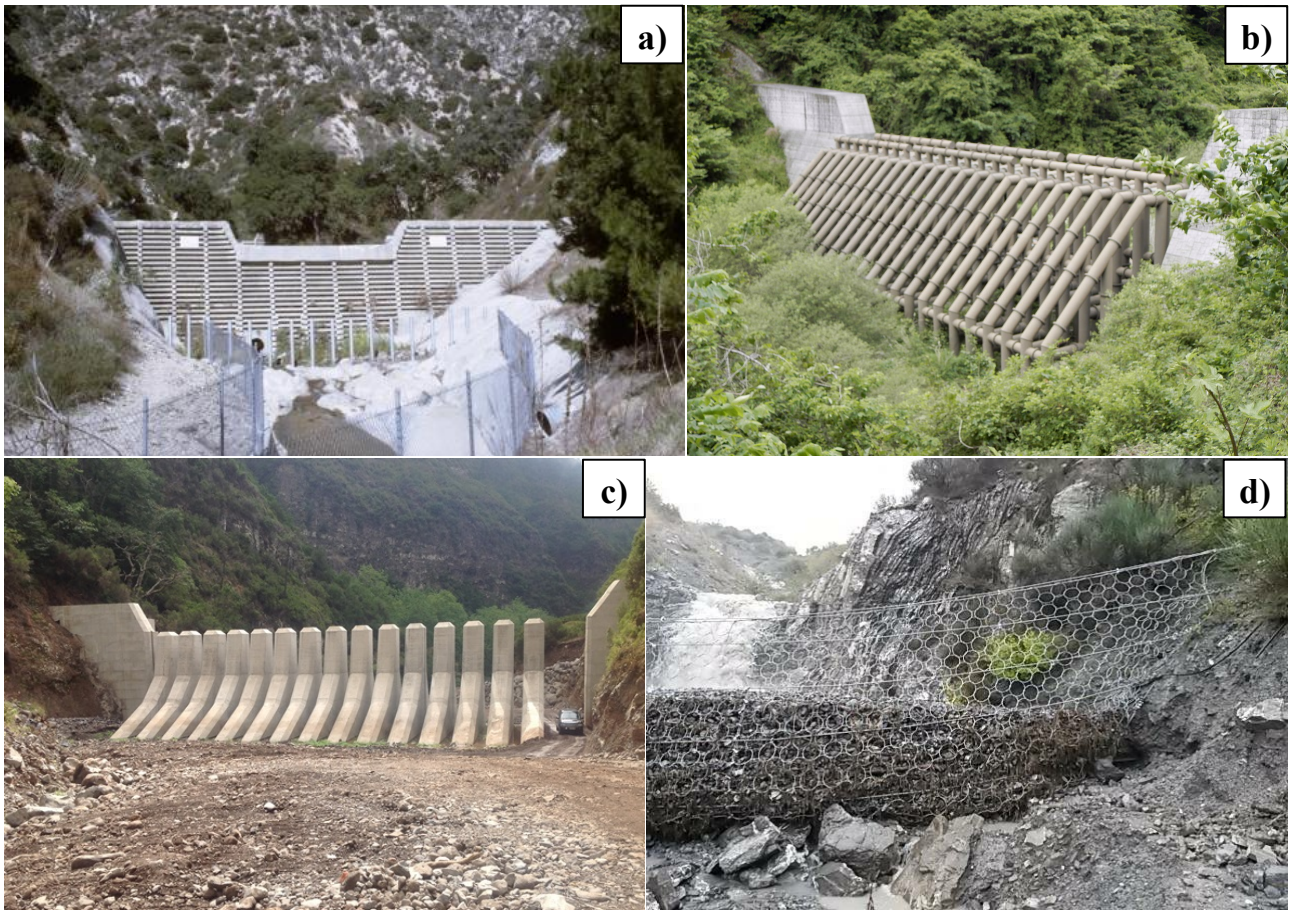

874

875 **Fig. 1** Different types of debris flow active mitigation measures: check dam (photograph by Los Angeles County Flood
876 Control Distric) (a), open type sabo structures (photograph of steel check dam in Nagano prefecture, Japan) (b),
877 concrete slit barrier (photograph by LCW Consult web site of protection works in St. Luzia River, Madeira, Portugal)
878 (c) and flexible net barrier (photograph by Geovertical S.R.L web site of protection works in Terranova Pollino,
879 Basilicata Region, Italy) (d).

880

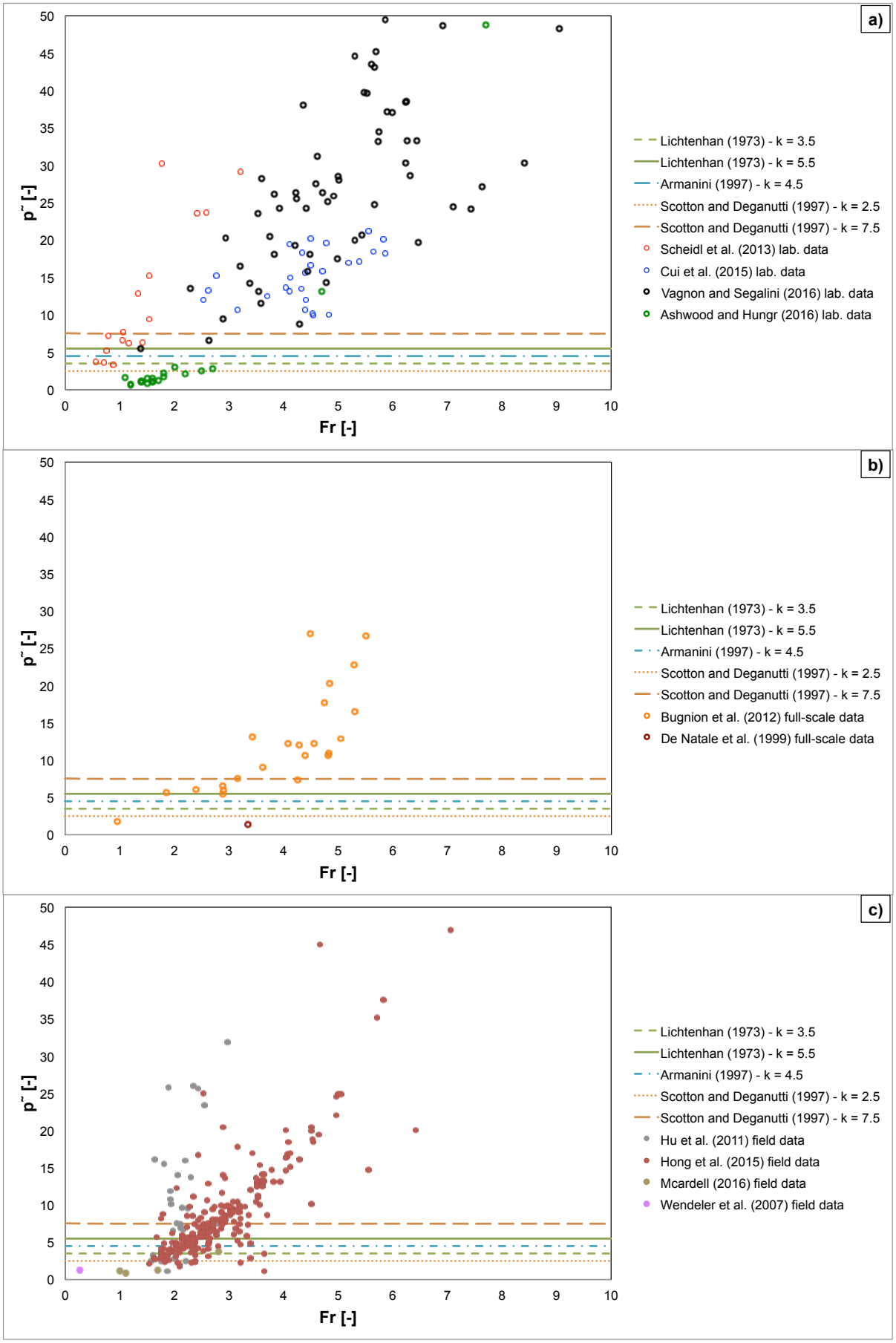

Fig. 2 Comparison between normalized debris flow impact force and hydro-static predicting models as function of Froude number considering small- (a) and full-scale experiments (b) and field data (c).

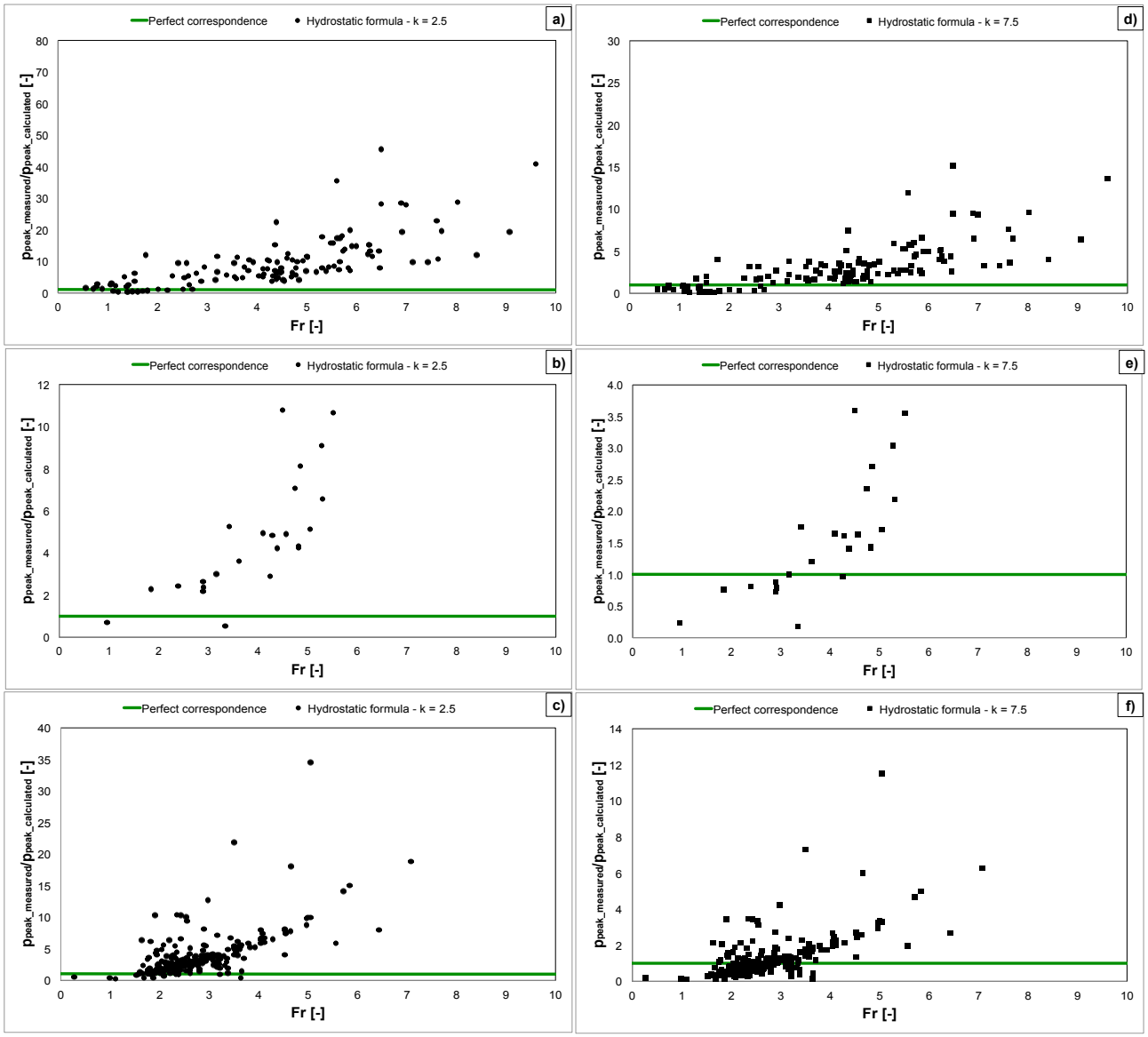

884

885 **Fig. 3** Relationship between measured peak pressure and calculated hydro-static peak pressure with k respectively equal
886 to 2.5 (a, to c) and 7.5 (d to f) as a function of the Froude number considering both small- (a, d) and full- scale (b, e) and
887 field dataset (c, f). The green continuous line represents the perfect correspondence between measured values and
888 estimated ones.

889

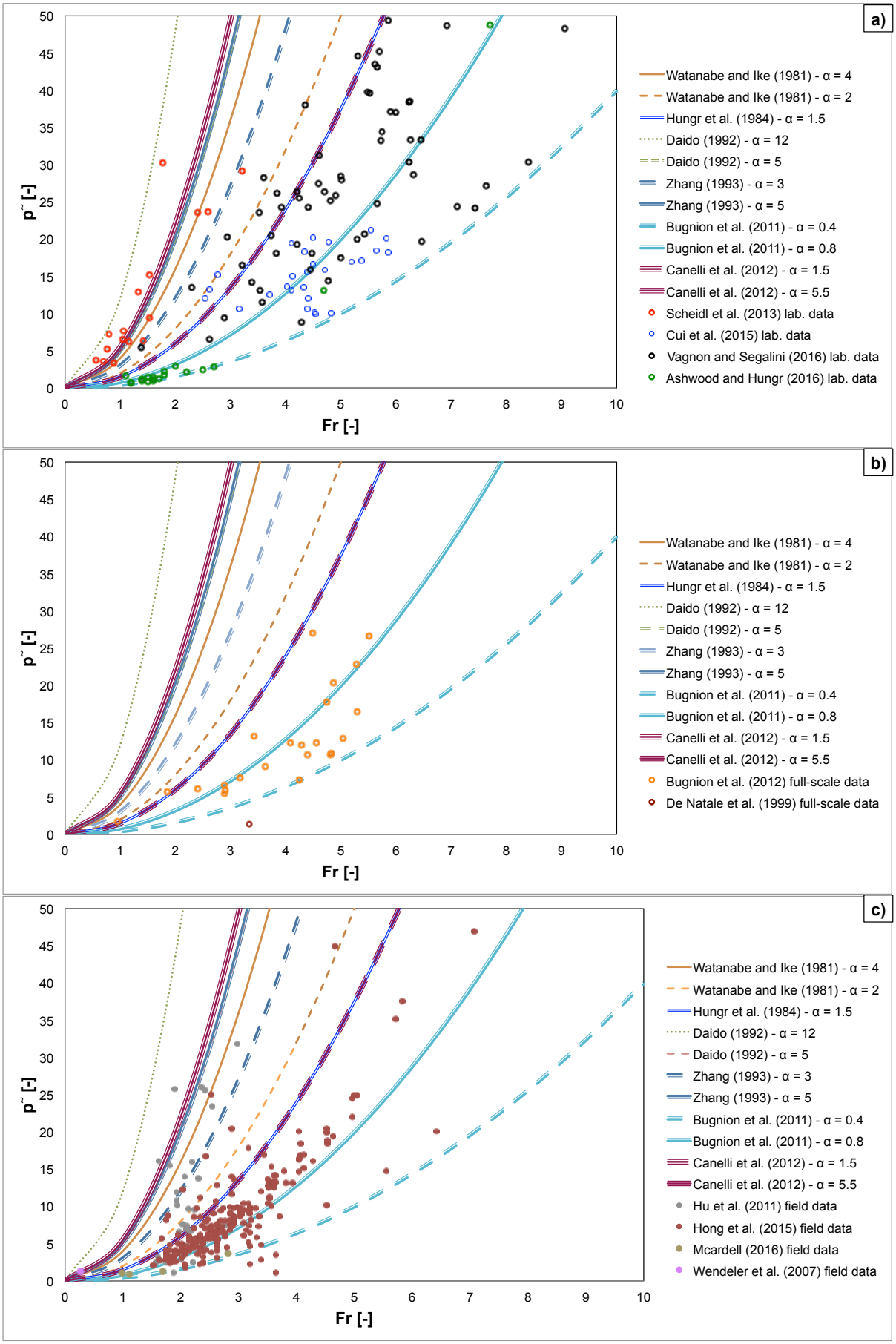

Fig. 4 Comparison between normalized debris flow impact force and hydro-dynamic predicting models as function of Froude number considering small- (a) and full-scale tests (b) as well as field data (c).

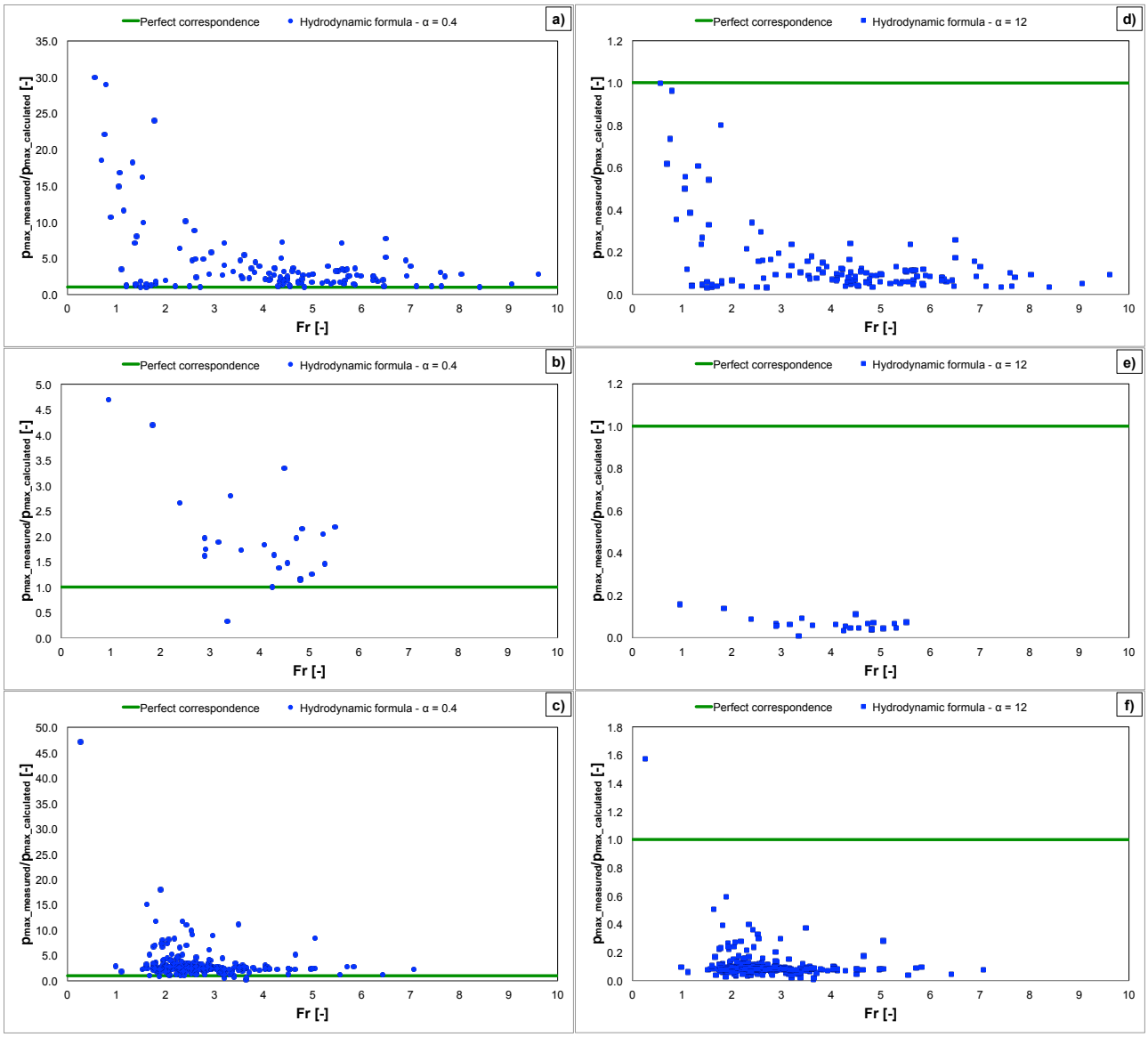

Fig. 5 Relationship between measured peak pressure and calculated hydro-dynamic peak pressure with α respectively equal to 0.4 (a to c) and 12 (c to d) as a function of the Froude number considering both small- (a, d) and full-scale (b, e) and field dataset (c, f).

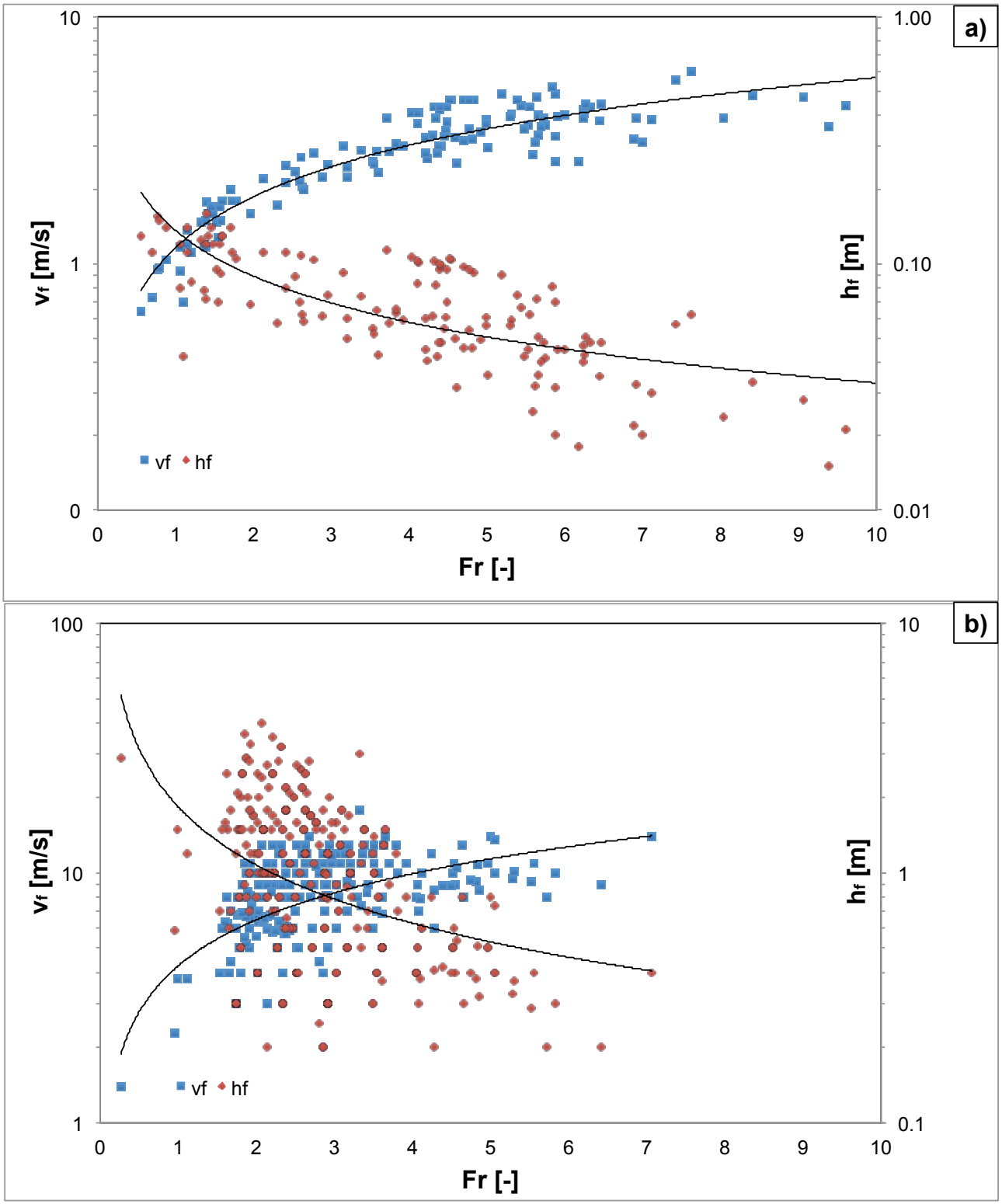

Fig. 6 Relationship between velocity (blue squares) and thickness (red diamonds) as function of Froude number for small-scale tests (a) and full-scale and field data (b). A negative correlation exists between velocity and thickness: when Froude number increases, velocity increases and consequently flow height decreases and vice-versa.

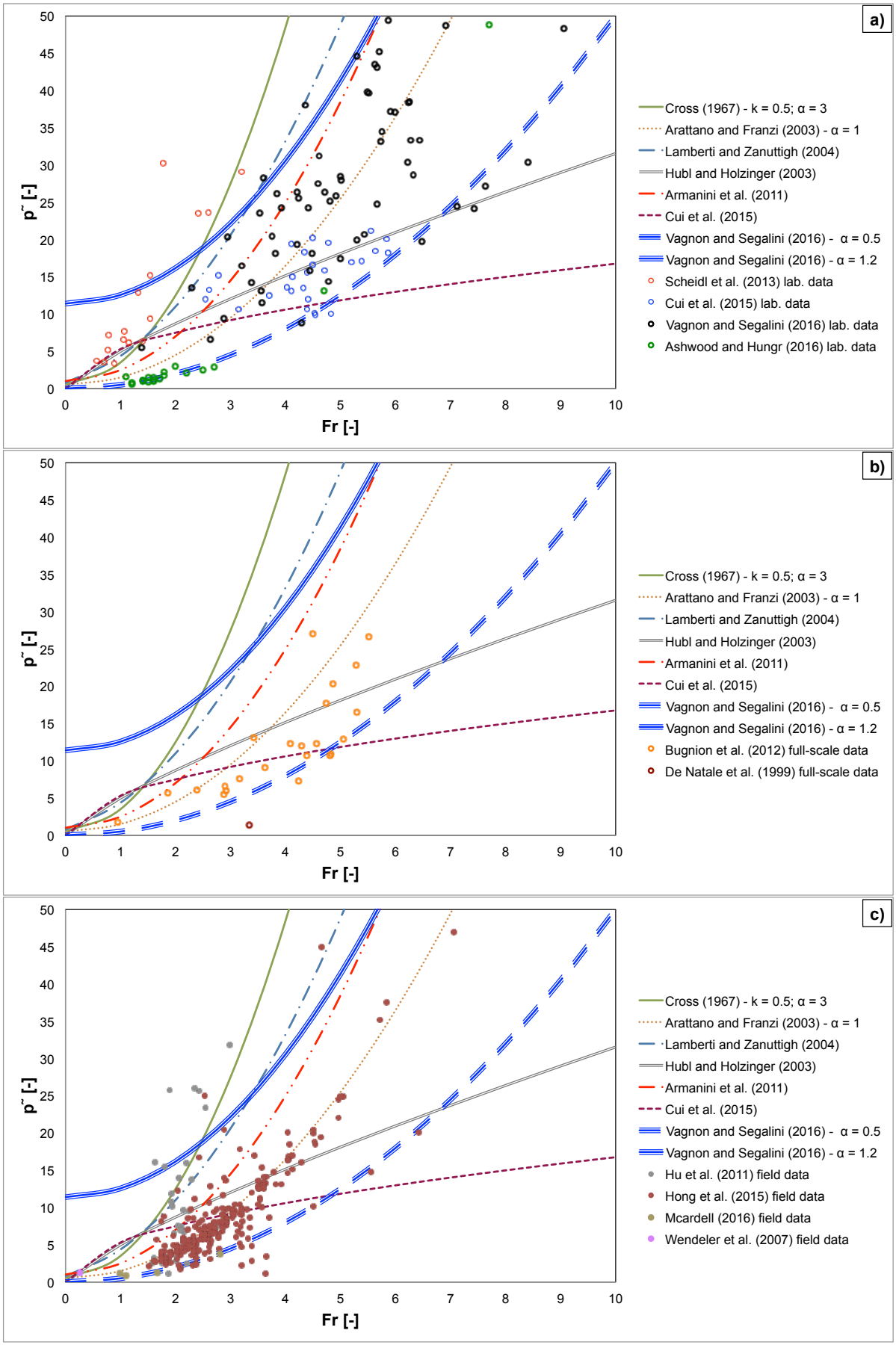

Fig. 7 Comparison between normalized debris flow impact force and mixed predicting models as function of Froude number considering small- (a) and full-scale test (b) as well as field data (c).

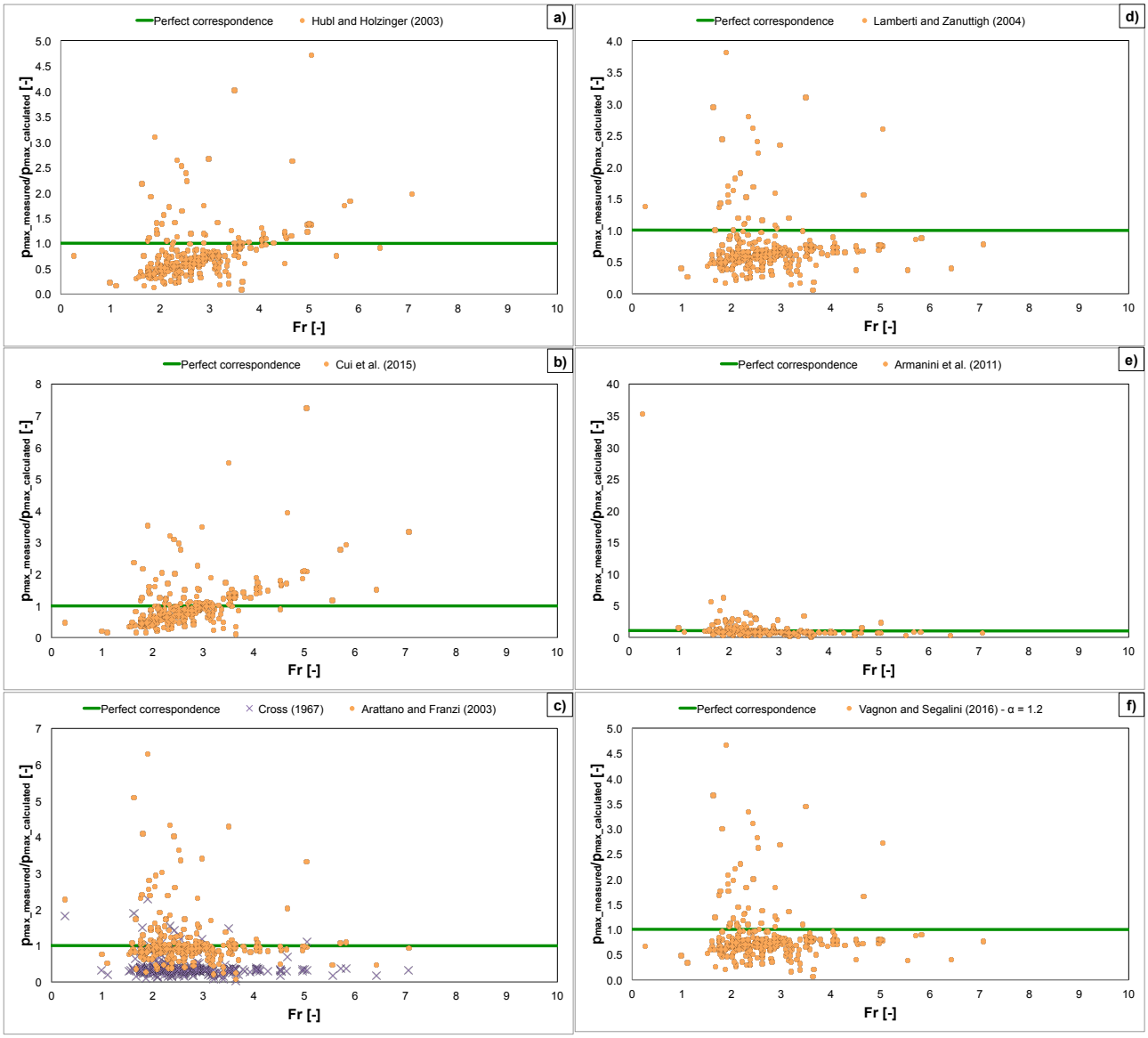

Fig. 8 Relationship between measured peak pressure and calculated peak pressure for different mixed models as a function of the Froude number considering field dataset (a to f).

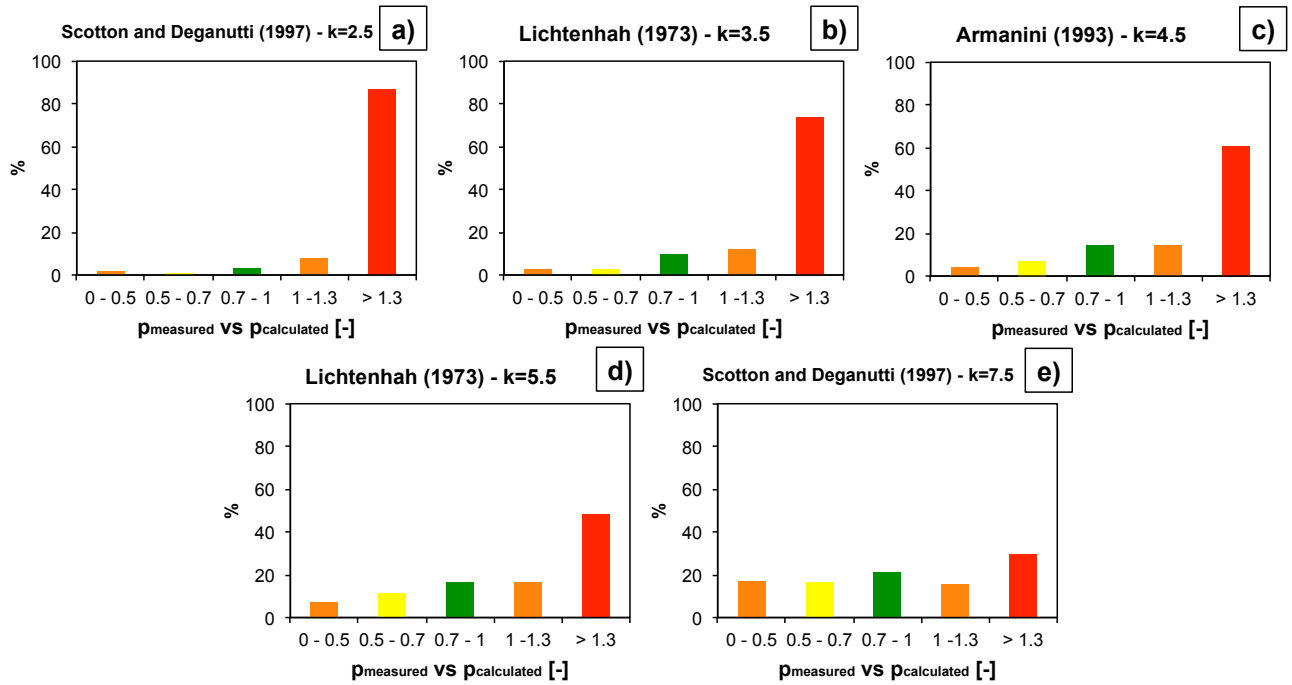

910

911 **Fig. 9** Predicting capability analysis of hydro-static models using field dataset.

912

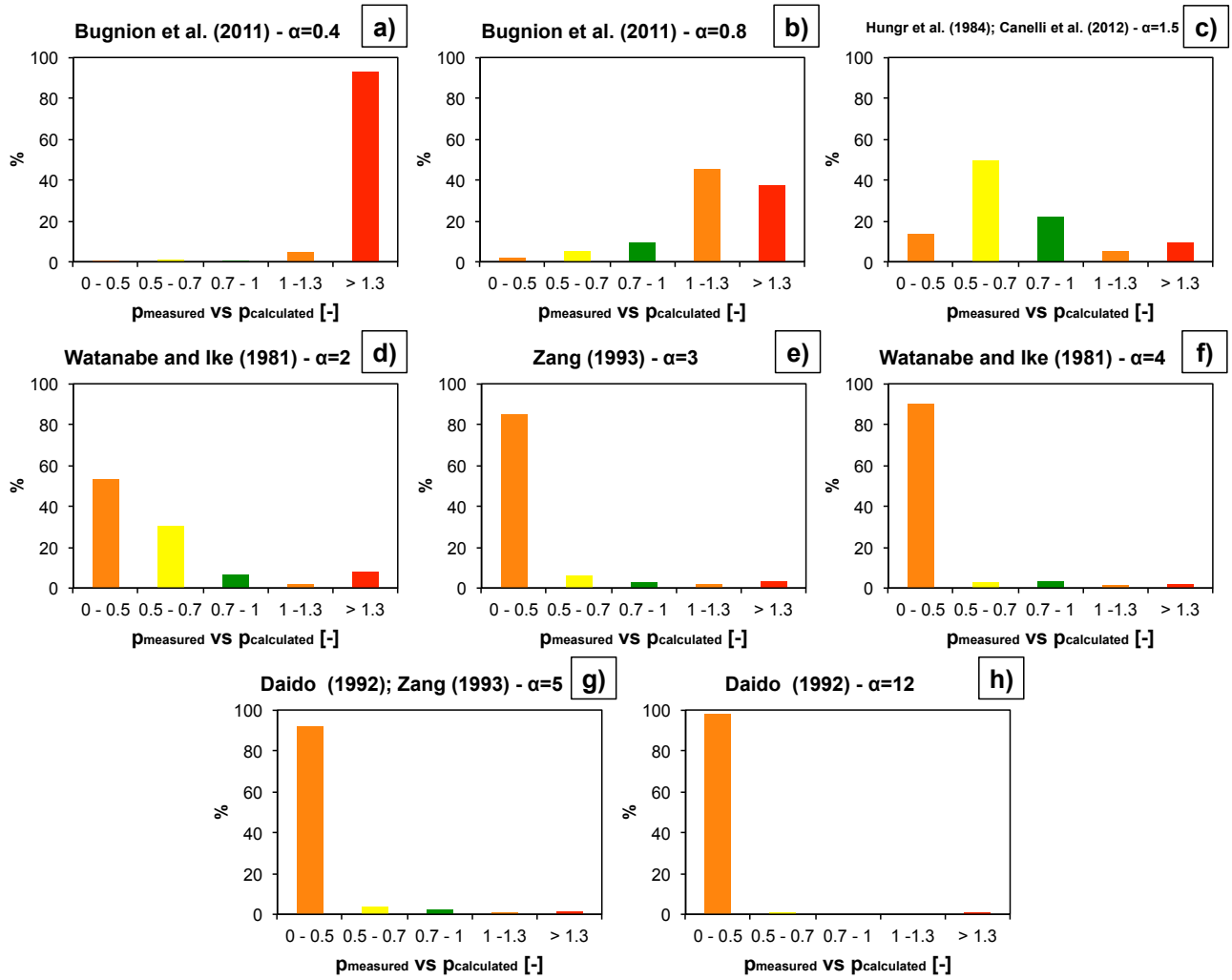

Fig. 10 Predicting capability analysis of hydro-dynamic models using field dataset.

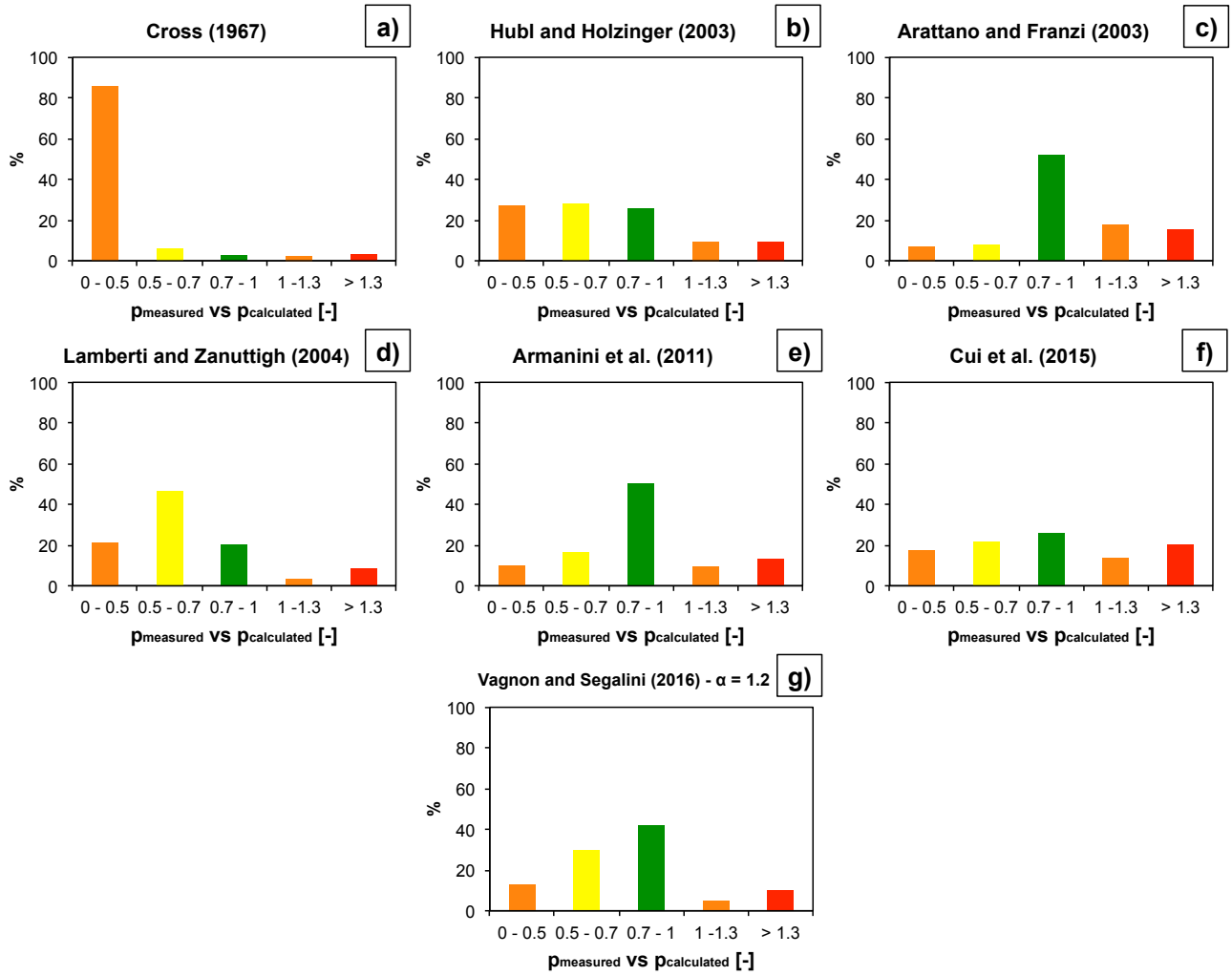

916

917 **Fig. 11** Predicting capability analysis of mixed models using field dataset.

918

919

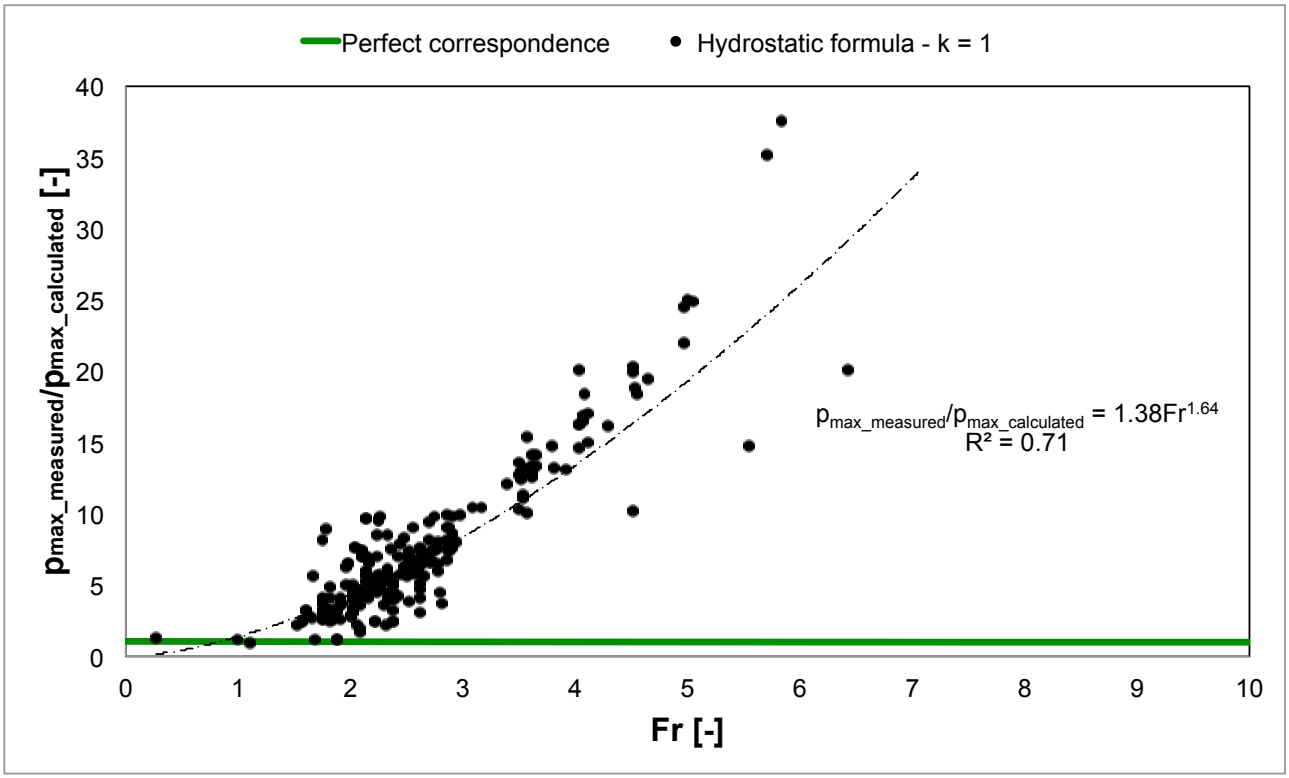

Fig. 12 Relationship between field measurements of the peak pressure and calculated peak pressure using hydro-static formulation with k=1 as a function of the Froude number of the flow.

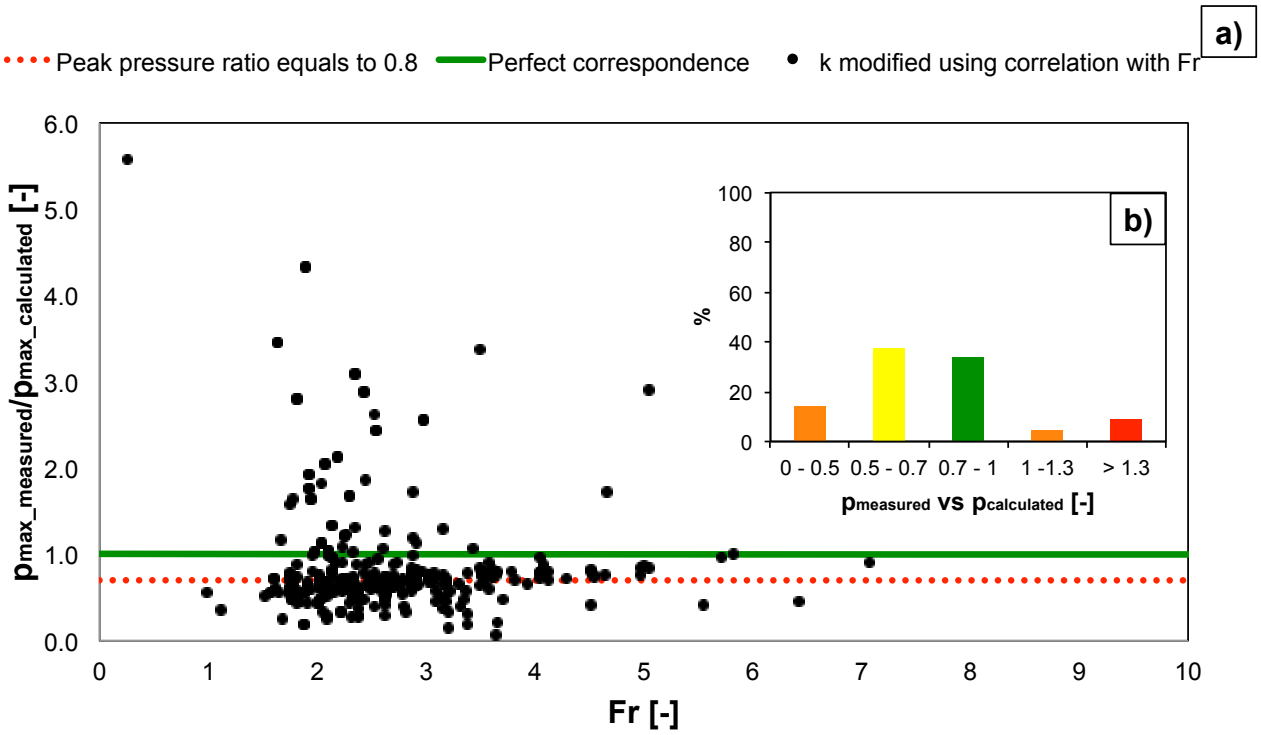

924

925 **Fig. 13** Relationship between peak pressure ratio for the modified hydro-static model as a function of the Froude
926 number (a) and statistical evaluation of the predicting capability of the proposed model (b).

927

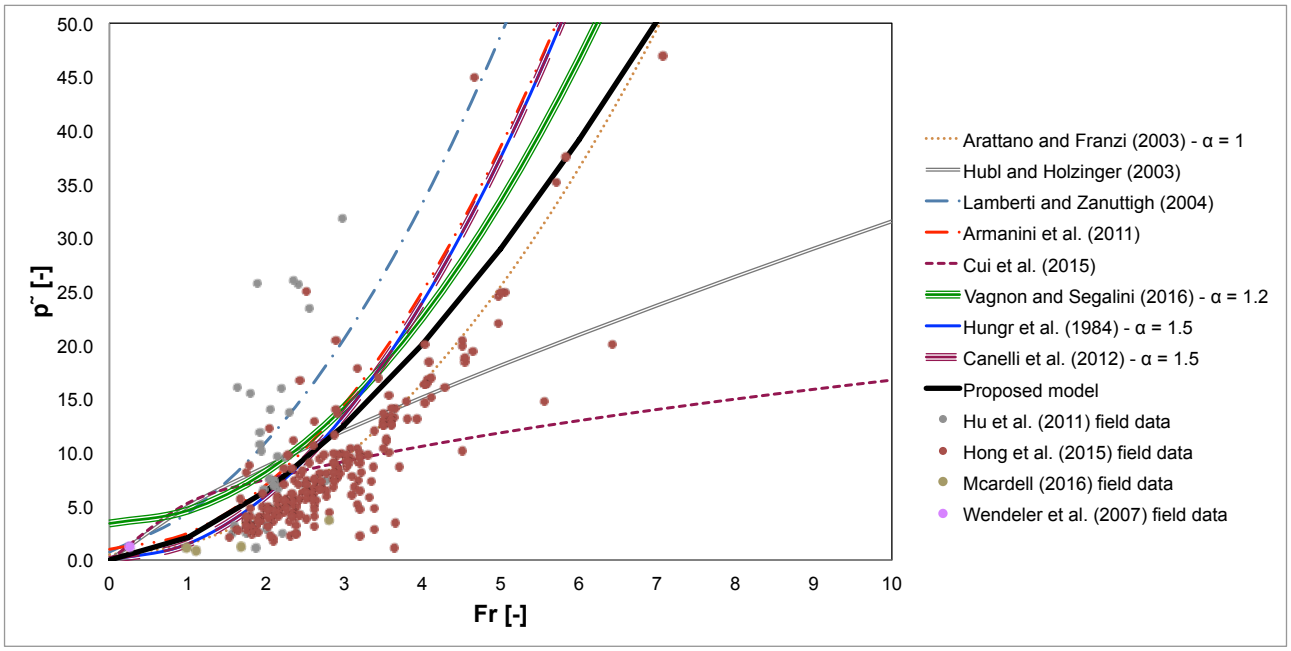

928

929 **Fig. 14** Comparison between the proposed model (black line) and others hydro-dynamic (Hungr et al. 1984 and Canelli
930 et al. 2012) and mixed (Arattano and Franzi 2003, Huebl and Holzinger 2003, Lamberti and Zanuttigh 2004, Armanini
931 et al. 2011, Cui et al. 2015 and Vagnon and Segalini 2016) models.